

Phase transitions in hexagonal, graphene-like lattice sheets and nanotubes under the influence of external conditions

D. Ebert^a, K.G. Klimenko^b, P.B. Kolmakov^{c,*}, V.Ch. Zhukovsky^c

^a*Institute of Physics, Humboldt-University Berlin, 12489 Berlin, Germany*

^b*State Research Center of Russian Federation – Institute for High Energy Physics, NRC "Kurchatov Institute", 142281, Protvino, Moscow Region, Russia*

^c*Faculty of Physics, Moscow State University, 119991, Moscow, Russia*

Abstract

In this paper we consider a class of (2+1)D schematic models with four-fermion interactions that are effectively used in studying condensed-matter systems with planar crystal structure, and especially graphene. Symmetry breaking in these models occurs due to a possible appearance of condensates. Special attention is paid to the symmetry properties of the appearing condensates in the framework of discrete chiral and C , \mathcal{P} and \mathcal{T} transformations. Moreover, boundary conditions corresponding to carbon nanotubes are considered and their relations with the effect of an applied external magnetic field are studied. To this end we calculated the effective potential for the nanotube model including effects of finite temperature, density and an external magnetic field. As an illustration we made numerical calculations of the chiral symmetry properties in a simpler Gross–Neveu model with only one condensate taken into account. We also investigated the phase structure of the nanotube model under the influence of the Aharonov–Bohm effect and demonstrated that there is a nontrivial relation between the magnitude of the Aharonov–Bohm phase, compactification of the spatial dimension and thermal restoration of the originally broken chiral symmetry.

Keywords: effective Lagrangian, phase transitions, carbon nanotubes, Zeeman effect, Aharonov–Bohm effect

PACS: 73.22.Gk, 11.10.Wx, 71.70.Ej

1. Introduction

It is a well-known fact that relativistic quantum field theory provides a powerful tool for the description of low-energy excitations in condensed-matter physics [1]. Examples are the field theoretic description of low-energy electron states in polymers [2, 3, 4] or the recent quasirelativistic treatment of electrons in planar systems like graphene, a single layer of graphite [5]. Recall that in the case of graphene, the original nonrelativistic tight-binding model for electrons on a hexagonal “honeycomb” lattice admits a low-momentum expansion around the two inequivalent “Dirac points”, the corners (valleys) of the first Brillouin zone, which leads to a linear dispersion law for low-energy fermion

*Corresponding author

Email address: pavel.b.kolmakov@yandex.ru (P.B. Kolmakov)

excitations, closely resembling that of massless relativistic Dirac fermions [5, 6]. Combining the two valley degrees of freedom with the two sublattice (pseudospin) degrees of freedom of electrons of carbon atoms, leads in a natural way to a reducible four-component Dirac spinor description in $D=(2+1)$ dimensions. It is just this property which allows for the introduction of a chiral γ_5 -matrix and the use of a chiral (Weyl) representation of Dirac matrices [7]. In the continuum limit, the free Dirac Lagrangian of graphene develops an emergent chiral "valley-sublattice" $U(2)_{vs}$ symmetry, which, when considering "multilayer" graphene with N_f flavors, is further enlarged to a chiral $U(2N_f)$ symmetry. There arises then the important question, whether the inclusion of fermion interactions can lead to a dynamical breakdown of chiral symmetry with an associated dynamical fermion mass generation and a "semimetal-insulator" phase transition.

The phenomenon of a dynamical generation of a fermion mass on the basis of a generic four-fermion interaction is well-known for strong interactions since the time, when Nambu and Jona-Lasinio (NJL) [8] generalized the BCS-Bogoliubov theory [9, 10] of superconductivity to a relativistic model with dynamical breaking of a continuous γ_5 -symmetry. Later on, QCD-motivated NJL-type of models were shown to successfully describe the low-energy meson spectrum of quantum chromodynamics (QCD) [11]. Similar types of four-fermion models with a discrete γ_5 -symmetry have also been considered in lower dimensions $D=(1+1)$ by Gross and Neveu (GN) [12], where the four-fermion theory is renormalizable and asymptotic free, or for $D=(2+1)$ in refs. [13, 14]. In the latter case, the model is perturbatively nonrenormalizable but becomes renormalizable in the $1/N_f$ expansion [15].

Generally, four-fermion models provide a useful effective low-energy description of an underlying relativistic fundamental theory. This fact makes it further interesting to investigate their modifications under the influence of external conditions, such as temperature, chemical potential, external magnetic fields etc. [16, 17, 18, 19]. Note, on the other hand, that in condensed-matter physics such models are meant to be effective from the very beginning. Non-renormalizability makes here no additional problem due to the natural cutoff in the ultraviolet momentum region provided by the finite spacing between the elements of the polymer lattice. Obviously, one may expect that local four-fermion interactions play also an important role for the generation of a dynamical mass gap and quantum phase transitions in graphene [20, 21, 22]. Let us refer in this context also to the interesting investigations based on Schwinger-Dyson equations [23, 24], renormalization group flow equations [20] and functional renormalization group methods [25, 26].

The main aim of this paper is to continue investigations based on approximative local four-fermion interactions of fermions in a graphene-like hexagonal lattice. In particular, we shall apply the method of the effective potential and the mean-field approach to describe fermionic quasiparticles and excitonic bound states for graphene-like lattice sheets and nanotubes. Moreover, we shall investigate phase transitions under external conditions like temperature, chemical potential and Aharonov-Bohm (AB) magnetic fields [27].

The paper is organized as follows. In Sect. 2 we first review the effective low-energy model of N_f non-interacting fermion species (flavors) living on a planar honeycomb lattice. Particular attention is paid to the emergent chiral symmetry $U(2N_f)$. Next, we will consider possible $U(2N_f)$ -invariant effective four-fermion interactions obtained by

a contact approximation of the instantaneous Coulomb potential using the “braneworld” or “reduced QED scenario” proposed in ref. [28]. In this approach fermions are localized on a 2D brane and move with Fermi velocity v_F , whereas the electromagnetic gauge field propagates in the 3D bulk with speed of light c . In graphene one has $v_F/c \approx 1/300$, so that the effective fine-structure constant is $\alpha_{\text{eff}} = \alpha c/v_F \approx 2$ ($\alpha = 1/137$), providing us with an interesting strong coupling theory. Next, the obtained four-fermion Coulomb-based interaction is projected by a Fierz-transformation into the fermion-hole channels, where exciton bound states can occur. This results in an effective NJL-type of interactions which keeps the global $U(2N_f)$ symmetry intact. However, one cannot postulate exact chiral $U(2N_f)$ symmetry from the very beginning. The reason is that chiral symmetry arises only in the continuum limit and is not exact in the tight-binding lattice Hamiltonian [29, 30]. This requires to admit additional small on-side repulsive interaction terms which break the symmetry explicitly [23, 31]. By this reason, we finally omit all possible symmetry constraints between four-fermion couplings and start with a general schematic GN-type of model, considered in earlier papers [17, 32] for (2+1)D QED and QCD. Although not directly related to graphene, their methods turn out to be useful for our mathematical investigations. Finally, we also quote the symmetry breaking properties of fermion condensates concerning discrete \mathcal{P} , \mathcal{C} , \mathcal{T} , γ_5 and γ_3 transformations.

In Sect. 3 we perform the path-integral derivation of the effective potential in the large N_f (mean field) approximation. The global minimum point of the effective potential then determines the fermion mass gap. In addition, we determine the exciton spectrum from the two-point 1PI Green functions (inverse propagators) of fluctuating exciton fields. Finally, for possible applications to nanotubes, we compactify one spatial direction rolling up the honeycomb lattice to a cylinder. In the resulting nanotubes we shall take into account the effects of finite temperature, chemical potential and of magnetic AB fields. The influence of the magnetic AB-effect on similar compactified fermion systems was recently studied in refs. [33, 34, 35, 36] (see also the 5D model [37]), and earlier in ref. [38] and in physics of carbon nanotubes in refs. [39, 40, 41].

In Sect. 4 we numerically investigate chiral phase transitions in nanotubes in the presence of finite temperature, chemical potential and the magnetic AB-phase ϕ . In particular, we present phase portraits in the (T, μ) , (β, L) and (ϕ, β) planes, where $\beta = 1/T$ and $L = 2\pi R$ (R is the cylinder radius).

Sect. 5 contains our summary and conclusions. Technical details of the Fierz transformation, of the investigation of the phase structure of the considered general schematic GN-type of model and of fermion loop calculations for exciton propagators are relegated to three appendices.

2. Effective low-energy model

2.1. Non-interacting fermions on a planar honeycomb lattice

It is well known that the hopping of fermions living on a graphene-like hexagonal “honeycomb” lattice can be described by the following tight binding Hamiltonian [42] (for reviews see refs. [5, 7])

$$H_0 = -t \sum_{\vec{r} \in B} \sum_{i=1,2,3} [\psi^{+Aa}(\vec{r} + \vec{\delta}_i) \psi^{Ba}(\vec{r}) + h.c.]. \quad (1)$$

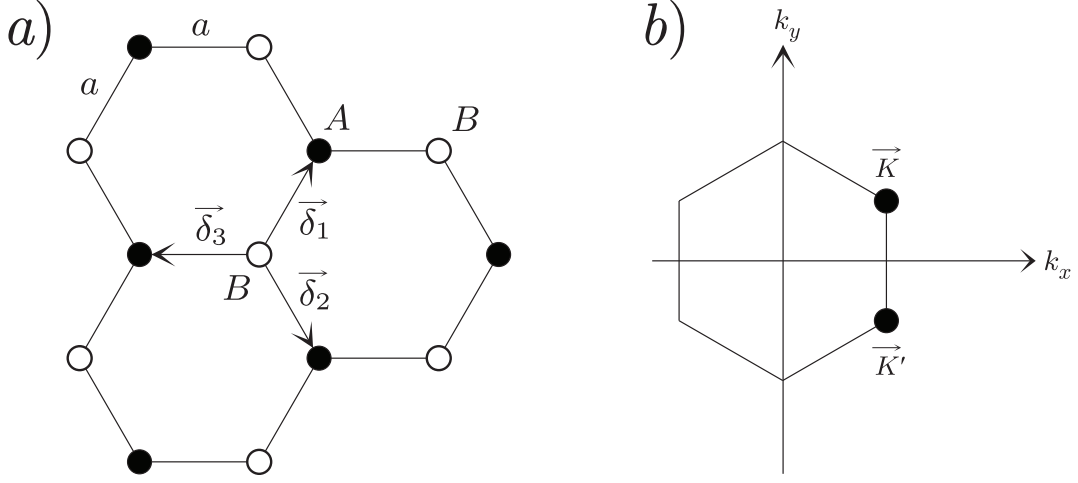


Figure 1: a.) Hexagonal honeycomb lattice with two interpenetrating triangular lattices of A and B sites. $\vec{\delta}_i$, $i = 1, 2, 3$ are the nearest neighbor vectors. b.) Corresponding Brillouin zone: the Dirac cones of the fermion spectrum are located at the K and K' points.

Here t is the nearest neighbor hopping parameter, ψ^{+Aa} and ψ^{Ba} are Fermi field operators belonging to triangular sublattices with A and B sites, and $\vec{\delta}_i$, $i = 1, 2, 3$ are three vectors directed from a B site to three nearest neighbor A sites. They are given by (Fig. 1a) $\vec{\delta}_1 = \frac{a}{2}(1, \sqrt{3})$, $\vec{\delta}_2 = \frac{a}{2}(1, -\sqrt{3})$, $\vec{\delta}_3 = -a(1, 0)$ with a being the distance between lattice sites.

For later use of a $1/N_f$ expansion, we consider here the "multilayer" case of $N_f = 2N$ degenerate fermion species (flavors) of real spin \uparrow and \downarrow , living on N hexagonal monolayers which are described by fields with a flavor index $a = (1, \dots, N_f = 2N)$. The monolayer case $N_f = 2$ corresponds to a fermion with two spin projections. Note that repeated indices a in eq. (1) have to be summed over and will be generally omitted.

In momentum representation, the Hamiltonian becomes diagonal,

$$H_0 = \sum_{\vec{k}} \left[\Phi(\vec{k}) \psi^{+Aa}(\vec{k}) \psi^{Ba}(\vec{k}) + h.c. \right], \quad \Phi(\vec{k}) = -t \sum_{\vec{\delta}_i} e^{-i\vec{k}\vec{\delta}_i}. \quad (2)$$

The energy bands, derived from this Hamiltonian are [6]

$$\mathcal{E}_{\pm}(\vec{k}) = \pm |\Phi(\vec{k})|, \quad (3)$$

where the $+/-$ signs refer to the upper/lower bands. It is important that there exist two inequivalent points K and K' ("Dirac points") at the corners of the first Brillouin zone, where $\mathcal{E}_{\pm}(\vec{K}; \vec{K}') = 0$. Their positions in the momentum space is given by (Fig. 1b)

$$\vec{K} = \left(\frac{2\pi}{3a}, \frac{2\pi}{3\sqrt{3}a} \right), \quad \vec{K}' = \left(\frac{2\pi}{3a}, -\frac{2\pi}{3\sqrt{3}a} \right). \quad (4)$$

Performing a low-momentum expansion of the energy spectrum (3) around the Dirac points, $\vec{k} = \vec{K}(\vec{K}') + \vec{p}$, with $|\vec{p}|a < 1$, one obtains the famous linear dispersion law $\mathcal{E}_{\pm} = \pm v_F |\vec{p}|$ for massless quasiparticles on the honeycomb

lattice¹. Here $v_F = \frac{3}{2}ta$ is the Fermi velocity with a being the lattice spacing. Transforming the low-momentum expansion of the Hamiltonian (2) back to configuration space gives in the continuum limit the Dirac-like free Hamiltonian (see e.g. refs. [5, 43])

$$H_0 = - \sum_{\eta=\pm 1} \sum_{a=1}^{N_f} \int d^2x \psi_{\eta}^{+a}(\vec{r}) \left[v_F \tau^1 i \partial_x + \eta v_F \tau^2 i \partial_y \right] \psi_{\eta}^a(\vec{r}), \quad (5)$$

where τ^i are 2×2 Pauli matrices. The Fermi operators $\psi_{\eta}^a(\vec{r})$ ($\vec{r} = (x, y)$) are two-spinors

$$\psi_{\eta}^a(\vec{r}) = \begin{pmatrix} \psi_{\eta}^{Aa} \\ \psi_{\eta}^{Ba} \end{pmatrix} \quad (6)$$

with indices A, B denoting sublattice ("pseudospin") degrees of freedom, and the subscript $\eta = \pm 1$ ("valley index") stands for the two Dirac points K, K' corresponding to valleys of the energy spectrum at the corners of the first Brillouin zone.

In what follows we shall be interested in the spontaneous breakdown of chiral symmetry which requires the existence of a chiral γ^5 -matrix. Such a matrix can only be obtained by using a reducible 4×4 representation of Dirac matrices.

Following Gusynin et al. [7], it is convenient to use the reducible chiral (Weyl) representation

$$\gamma^0 = \begin{pmatrix} 0 & \mathbf{I}_2 \\ \mathbf{I}_2 & 0 \end{pmatrix}, \quad \gamma^1 = \begin{pmatrix} 0 & -\tau^1 \\ \tau^1 & 0 \end{pmatrix}, \quad \gamma^2 = \begin{pmatrix} 0 & -\tau^2 \\ \tau^2 & 0 \end{pmatrix} \quad (7)$$

with \mathbf{I}_2 being the 2×2 unit matrix. There exist two more 4×4 matrices which anticommute with all γ^{μ} , $\mu = 0, 1, 2$ and with each other

$$\gamma^3 = \begin{pmatrix} 0 & -\tau^3 \\ \tau^3 & 0 \end{pmatrix}, \quad \gamma^5 = \begin{pmatrix} \mathbf{I}_2 & 0 \\ 0 & -\mathbf{I}_2 \end{pmatrix}, \quad (8)$$

as well as their combination

$$\gamma^{35} = \frac{1}{2} [\gamma^3, \gamma^5] = \begin{pmatrix} 0 & \tau^3 \\ \tau^3 & 0 \end{pmatrix}, \quad (9)$$

which commutes with all γ^{μ} , but anticommutes with γ^3 and γ^5 . Note that ($\mu = 0, 1, 2, 3$)

$$\{\gamma^{\mu}, \gamma^{\nu}\} = 2g^{\mu\nu} \mathbf{I}_4, \quad g^{\mu\nu} = \text{diag}(1, -1, -1, -1), \quad (10)$$

where \mathbf{I}_4 is the 4×4 unit matrix. Let us now replace the operator-valued fields by 4-spinor Grassmann fields

$$\psi^t = \left(\psi_K^{Aa}, \psi_K^{Ba}, -i\psi_{K'}^{Ba}, i\psi_{K'}^{Aa} \right), \quad (11)$$

where t stands for the transposition operation.

¹ In this paper we use natural units $\hbar = c = k_B = 1$, where k_B is the Boltzmann constant. Obviously, the Fermi velocity v_F is then also dimensionless.

By using the notations $\psi_\eta^{A,B} \equiv \psi_{K,K'}^{A,B}$ for $\eta = \pm 1$, one can reexpress the Hamiltonian (5) in a convenient 4-spinor notation. With $\bar{\psi}^a = \psi^{+a}\gamma^0$, one arrives at the effective free low-energy Lagrangian

$$L_0 = \bar{\psi} \left[i\gamma^0 \partial_0 + iv_F \gamma^1 \partial_x + iv_F \gamma^2 \partial_y \right] \psi = \bar{\psi} i\gamma^\mu \tilde{\partial}_\mu \psi, \quad (12)$$

where $\tilde{\partial}_\mu = (\partial_0, v_F \vec{\nabla})$, using notations $x^0 = t$, $\partial_0 = \partial_t$, and implicit summation over the flavor index a is understood.

It is illuminative to introduce also chiral projection operators $\mathcal{P}_\pm = \frac{1}{2}(1 \pm \gamma^5)$ and "right" and "left" spinors $\psi_\pm = \mathcal{P}_\pm \psi$, i.e.

$$\psi_+ = \begin{pmatrix} \psi_K^{Aa} \\ \psi_K^{Ba} \\ 0 \\ 0 \end{pmatrix}, \quad \psi_- = \begin{pmatrix} 0 \\ 0 \\ -i\psi_{K'}^{Ba} \\ i\psi_{K'}^{Aa} \end{pmatrix}, \quad (13)$$

so that

$$\gamma^5 \psi_\pm = \pm \psi_\pm. \quad (14)$$

In the chiral representation of Dirac matrices, the fermion excitations at the two distant Dirac points K, K' ($\eta = \pm 1$), corresponding to spinors ψ_\pm , thus turn out to be states of definite chirality eigenvalues ± 1 . Obviously, the latter coincide with the values of the valley index $\eta = \pm 1$ ².

2.2. Symmetry properties

It is straightforward to see that the matrices γ^3, γ^5 and γ^{35} together with the 4×4 unit matrix I_4 are generators of an emergent global continuous "valley-sublattice" symmetry $U(2)_{vs} = U(1)_{vs} \times SU(2)_{vs}$ [7]. Indeed, it is easy to see that the three generators

$$t^1 = \frac{1}{2}i\gamma^3, \quad t^2 = \frac{1}{2}\gamma^5, \quad t^3 = \frac{1}{2}\gamma^{35} \quad (15)$$

commute with the free Lagrangian (12) and satisfy the $SU(2)$ algebra

$$[t^i, t^j] = i\varepsilon_{ijk} t^k, \quad (16)$$

where ε_{ijk} is the Levi-Civita symbol. Moreover, let us introduce the $U(1)$ -generator $t^0 = \frac{1}{2}I_4$. Then we have the normalization $\text{tr } t^i t^j = \delta^{ij}$, where $i, j = 0, \dots, 3$. Clearly, one may also consider special continuous $U(1)_{t^k}$ transformations ($k = 0, \dots, 3$), related to the generators t^k in eq. (15) and to the generator t^0 ,

$$U(1)_{t^k} : \psi \rightarrow e^{i\alpha_k t^k} \psi, \quad \bar{\psi} \rightarrow \bar{\psi} e^{-i\alpha_k t^k}, \quad (17)$$

² Note that the chirality eigenvalues coincide with the eigenvalues of the helicity operator $\Lambda_p = \frac{\vec{p} \cdot \vec{\Sigma}}{|\vec{p}|}$, where $\vec{\Sigma} = \text{diag}(\vec{\tau}, \vec{\tau})$ is the pseudospin.

where $s_k = -1$ for $k = 1, 2$ and $s_k = 1$ for $k = 0, 3$. In addition to the above $U(2)_{v_s}$ valley-sublattice symmetry, the Lagrangian (12) exhibits invariance under the global group $U(N_f)$ of flavor symmetry. In fact, it is invariant under the larger group $U(2N_f)$, spanned by the generators given by the direct products

$$t^i \otimes \frac{\lambda^\alpha}{2} \otimes \frac{\sigma^m}{2} \quad i = (0, \dots, 3), \alpha = (0, \dots, N^2 - 1), m = (0, \dots, 3), N_f = 2N, \quad (18)$$

with λ^α ($\alpha = 0, \dots, N^2 - 1$) being generalized Gell-Mann matrices of $U(N)$ with $\text{tr} \lambda^\alpha \lambda^\beta = 2\delta^{\alpha\beta}$, $\lambda^0 = \sqrt{\frac{2}{N}}\mathbf{I}_N$, and σ^m are the Pauli spin matrices ($\sigma^0 = \mathbf{I}_2$) of the spin rotation group $U(2)_s$.

For later use, let us also quote the transformation laws of 4-spinors under the discrete symmetries: inversion of x -coordinate \mathcal{P} , charge conjugation \mathcal{C} , and time reversal \mathcal{T} ,

$$\begin{aligned} \psi(x^0, x, y) &\xrightarrow{\mathcal{P}} i\gamma^1\gamma^5\psi(x^0, -x, y), \\ \psi(x^0, \vec{r}) &\xrightarrow{\mathcal{C}} \gamma^1\bar{\psi}^t(x^0, \vec{r}), \\ \psi(x^0, \vec{r}) &\xrightarrow{\mathcal{T}} i\sigma^2\gamma^1\gamma^5\psi(-x^0, \vec{r}) \end{aligned} \quad (19)$$

where σ^2 acts on the spin indices of the spinor.

2.3. Effective four-fermion interactions

2.3.1. Contact approximation of electromagnetic interactions

As usual, electromagnetic interactions between quasiparticles are introduced into the free Lagrangian L_0 of eq. (12) by covariant derivatives $\tilde{\partial}_\mu \rightarrow \tilde{D}_\mu = (\partial_0 - ieA_0, v_F(\vec{\nabla} + ie\vec{A}))$. Let us consider here the "braneworld" or "reduced" QED-scenario proposed in ref. [28] and start with the Dirac-Maxwell action ³

$$S = \int d^3x \bar{\psi} i\gamma^\mu \tilde{D}_\mu \psi - \frac{\varepsilon_0}{4} \sum_{\mu, \nu=(0, \dots, 3)} \int d^4x F_{\mu\nu} F^{\mu\nu}. \quad (20)$$

Here the fermionic quasiparticles run in the (2+1)-dimensional space-time $x^{(3)} = (x^0, x^1, x^2)$ with Fermi velocity v_F , while the $U(1)$ gauge field A^μ propagates in (3+1)-dimensional bulk space-time $x^{(4)} = (x^0, x^1, x^2, x^3)$ with the speed of light $c(=1)$. Notice that the gauge field appearing in the covariant derivative $\tilde{\partial}_\mu \rightarrow \tilde{D}_\mu$ is taken on the plane $x^3 = 0$.

The gauge coupling constant e ($-e < 0$) is the electric charge for the vacuum-suspended honeycomb lattice, and ε_0 is the dielectric constant of the vacuum. If the layer is placed on a substrate, the interaction strength is screened by the factor $2/(1 + \varepsilon)$ with ε being the dielectric constant of the substrate [45]. Let us slightly rewrite the action (20) in a form making the coupling of the gauge field to fermion charge and current densities ρ, \vec{j} explicit,

$$S = -\frac{\varepsilon_0}{4} \sum_{\mu, \nu=(0, \dots, 3)} \int d^4x F_{\mu\nu} F^{\mu\nu} + \int d^3x L_0 + \int d^3x [A_0 \rho - \vec{A} \cdot \vec{j}], \quad (21)$$

³ The electromagnetic vector potential \vec{A} can be introduced in the lattice Hamiltonian (1) with the Peierls' substitution, i.e. by introducing the phase factor $\exp(-ie\vec{\delta}_i \cdot \vec{A})$ into the hopping term [7]. In a similar way, the scalar potential can be obtained from changing the next-to-nearest hoppings [5, 44, 43].

with L_0 given in eq. (12), and

$$\rho = e\bar{\psi}\gamma^0\psi, \quad j^1 = ev_F\bar{\psi}\gamma^1\psi, \quad j^2 = ev_F\bar{\psi}\gamma^2\psi, \quad j^3 = 0. \quad (22)$$

As has been demonstrated in ref. [28], the action S can be further rewritten by introducing a new (2+1)-dimensional “brane” gauge field $A_\mu(x^0, x^1, x^2)$, ($\mu = 0, 1, 2$). The resulting effective action then takes the form

$$S = \int d^3x \left[- \sum_{\mu,\nu=(0,\dots,2)} \frac{\varepsilon_0}{2} F_{\mu\nu} \frac{1}{\sqrt{-\partial^2}} F^{\mu\nu} + L_0 + A_0\rho - \vec{A} \cdot \vec{j} + \text{gauge terms} \right] \quad (23)$$

with a nonlocal kinetic term of the gauge field. Finally, let us consider the partition function for the action (23),

$$Z = \int D\psi D\bar{\psi} D_\mu[A_\mu] \exp[iS], \quad (24)$$

where the path-integral measure $D_\mu[A_\mu]$ includes the gauge-fixing terms. For the following discussion it turns out convenient to reintroduce, for a moment, again the speed of light c . By integrating out the gauge field and neglecting relativistic corrections of order $(v_F/c)^2$ (for graphene we have $v_F/c \sim 1/300$), arising from currents \vec{j} , one obtains the following expression for the action containing Coulomb interactions of fermions on the lattice plane

$$S = S_0 - \frac{v_F}{2c} \int d^{(3)}x' \int d^{(3)}x [\bar{\psi}(x^0, \vec{r})\gamma^0\psi(x^0, \vec{r})] U_0^C(x^0 - x'^0, |\vec{r} - \vec{r}'|) [\bar{\psi}(x'^0, \vec{r}')\gamma^0\psi(x'^0, \vec{r}')]. \quad (25)$$

Here U_0^C is the bare instantaneous Coulomb potential which takes the form

$$U_0^C(x^0, |\vec{r}|) = \frac{e^2\delta(x^0)}{2\varepsilon_0v_F} \int \frac{d^2k}{(2\pi)^2} \exp(i\vec{k}\vec{r}) \frac{1}{|\vec{k}|} = \alpha \left(\frac{c}{v_F} \right) \frac{\delta(x^0)}{|\vec{r}|}, \quad (26)$$

where $\alpha = e^2/(4\pi\varepsilon_0c) \simeq 1/137$ is the fine-structure constant. Recall that for graphene $v_F/c \sim 1/300$, and the effective fine-structure constant in eq. (26) is $\alpha_{\text{eff}} = \alpha \frac{c}{v_F} \sim 2$. Thus, the honeycomb lattice provides us with an interesting strong-coupling theory.

It is worth noting that in the case of finite temperature, and/or finite density, polarization effects and a Debye screening mass may considerably modify the bare Coulomb potential [23, 46] leading to a full (non-perturbative) expression $U^C(x)$.

It should be noted that a great simplification in solving the Hartree-Fock (gap) equation for fermion masses and the Bethe-Salpeter equation for exciton bound states arises, if one approximately replaces the unknown full Coulomb potential $U^C(x)$ by a δ -function contact interaction. In particular, let us suppose that the photon propagator gets a non-perturbative effective photon mass M .⁴ In this case, the integral in eq. (26) is replaced by

$$\int \frac{d^2k}{(2\pi)^2} \exp(i\vec{k} \cdot \vec{r}) \frac{1}{\sqrt{\vec{k}^2 + M^2}} \xrightarrow{M^2 \gg \vec{k}^2} \frac{1}{M} \delta^{(2)}(\vec{r}). \quad (27)$$

Thus we get a “low-momentum” contact interaction

$$U^C(x) = \frac{2\pi\alpha}{M} \frac{c}{v_F} \delta^{(3)}(x) \equiv G_c \delta^{(3)}(x), \quad (28)$$

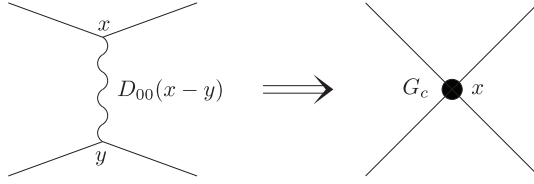


Figure 2: *Contact approximation to the non-local Coulomb interaction. The full photon propagator D_{00} is replaced by a local four-fermion interaction of strength G_c .*

with $G_c = \frac{2\pi\alpha}{M} \frac{c}{v_F}$ characterizing the effective interaction strength. The considered contact approximation (see Fig. 2) leads to the following $U(2N_f)$ -invariant four-fermion part of the interaction Lagrangian ⁵

$$L_{\text{int}}^C = -\frac{G_c v_F}{2} [\bar{\psi}(x)\gamma^0\psi(x)]^2. \quad (29)$$

Since the coupling constant G_c has mass dimension $[G_c] = -1$, a theory based on eq. (29) is not renormalizable in usual perturbation theory, but turns out to be renormalizable in the $1/N_f$ expansion.

In the following subsection we shall project the 4-fermion Coulomb-based interaction (29), motivated from photon exchange, by a Fierz transformation into fermion-hole channels, where bound exciton states occur. This results in an effective Nambu–Jona-Lasinio (NJL) type of interaction which keeps global chiral $U(2N_f)$ and fermion number $U(1)$ symmetries intact. It is well-known from strong interaction physics that NJL-type models [8] naturally incorporate the dynamical mechanism for spontaneous breakdown and restoration of chiral symmetry. As demonstrated for the case of QCD, an analogous contact approximation for the long-range gluon interaction between colored quark currents leads to a QCD-based NJL model which has been shown to give a successful description of fermion masses and coupling constants, as well as of masses of hadronic bound states [11, 48]. Based on such experience, one might expect that the contact interaction (29) and its resulting Fierz-transformed NJL-type terms might become, at least qualitatively, a reasonable starting point for a non-perturbative low-energy description of chiral symmetry breaking and restoration in graphene-like models.

It should be noted that the $U(2N_f)$ symmetry of the Lagrangian is broken, when a spin Zeeman interaction with an external magnetic field \mathbf{B} is included (comp. Section 2.3.3). Moreover, it is worth mentioning that the valley-sublattice symmetry $U(2)_{vs}$ is an emergent symmetry arising in the continuum limit, which is not exact in the tight-binding lattice Hamiltonian H_0 [29, 30]. By this reason, one cannot postulate that chiral $U(2N_f)$ invariance of the continuum Lagrangian L , corresponding to the action (25) or the contact Coulomb-like interaction (29), must hold for the complete effective Lagrangian, too.

⁴ Photon masses might, for example, arise from a Higgs mechanism with a Cooper pair condensate (Meissner effect) and/or from Debye screening. In the following, we shall consider M rather as the size of the low-energy region, where a contact approximation is applicable.

⁵ Clearly, due to suppression of spatial components of currents and associated retardation effects, the expression (29) is not Lorentz-invariant. It thus differs from the Thirring model with $v_F = c$ considered in refs. [47, 25].

In particular, the Coulomb interaction on the lattice contains additionally a small on-site repulsive interaction term [23, 31]

$$\Delta L_{\text{int}} = \frac{G_{\text{VF}}}{2} (\bar{\psi}\psi)^2, \quad (30)$$

which breaks the $U(2N_f)$ symmetry explicitly according to $U(2N_f) \rightarrow U(N_f)_{\rho} \otimes U(N_f)_{\beta}$. Here the groups $U(N_f)_i$ have the Lie algebra of eq. (18) with two unbroken generators t^0, t^3 .

Analogous terms may arise from phonon-mediated interactions with coupling strength g [39]. Combining the expressions (29) and (30) and including the phonon-mediated interaction term leads to the symmetry breaking interaction Lagrangian

$$L_{\text{int}} = -\frac{1}{2} G_{c,\text{VF}} (\bar{\psi}\gamma^0\psi)^2 + \frac{\tilde{G}_{\text{VF}}}{2} (\bar{\psi}\psi)^2, \quad (31)$$

where \tilde{G} is the effective coupling $\tilde{G} = G + g$.

2.3.2. Fierz-transformed interaction Lagrangian

In the following we shall study dynamically generated fermion masses (gaps) arising from condensates of exciton fields describing quasiparticle-hole bound states. This requires to project the interaction term (31) by a Fierz transformation into bound-state channels for exciton fields φ^A , $\varphi^A \sim \bar{\psi}\Gamma^A\psi$. Here Γ_A is a complete basis of the 4×4 Dirac algebra, given by the 16 matrices

$$\{\Gamma^A\}_{A=1}^{16} = \{\mathbb{I}_4, i\gamma^3, \gamma^5, \gamma^{35}, \tilde{\gamma}^\mu, \tilde{\gamma}^{\mu 3}, \tilde{\gamma}^{\mu 5}, \tilde{\gamma}^{\mu 35}\}, \quad (32)$$

where

$$\begin{aligned} \tilde{\gamma}^\mu &= (\gamma^0, i\gamma^k), & \tilde{\gamma}^{\mu 3} &= (\gamma^0\gamma^3, i\gamma^k\gamma^3), \\ \tilde{\gamma}^{\mu 5} &= (\gamma^0i\gamma^5, \gamma^k\gamma^5), & \tilde{\gamma}^{\mu 35} &= (\gamma^0\gamma^{35}, i\gamma^k\gamma^{35}), \quad (k = 1, 2) \end{aligned} \quad (33)$$

and we have $(\Gamma^A)^\dagger = \Gamma^A = (\Gamma^A)^{-1}$, $\text{Tr}\Gamma^A\Gamma^B = 4\delta^{AB}$.

Taking into account only NJL-type scalar/pseudoscalar interactions and discarding, for simplicity, axial/vector type terms, the Fierz transformation of the two terms in the interaction Lagrangian (31) gives (see Appendix A, eqs. (A.9) and (A.10)):

$$L_{\text{int}}^{F,C} = \frac{1}{2} \frac{G_{c,\text{VF}}}{4N_f} \left\{ [(\bar{\psi}\psi)^2 + (\bar{\psi}\gamma^3\psi)^2 + (\bar{\psi}i\gamma^5\psi)^2] + (\bar{\psi}\gamma^{35}\psi)^2 \right\} + \dots, \quad (34)$$

$$\Delta L_{\text{int}}^F = -\frac{1}{2} \frac{\tilde{G}_{\text{VF}}}{4N_f} \left\{ [(\bar{\psi}\psi)^2 - (\bar{\psi}\gamma^3\psi)^2 - (\bar{\psi}i\gamma^5\psi)^2] + (\bar{\psi}\gamma^{35}\psi)^2 \right\} + \dots \quad (35)$$

Moreover, since we shall consider only the condensates of flavor/spin-singlet excitons, we have taken into account only corresponding singlet terms in the completeness relations (A.4) and (A.5).

Notice that the first three terms in the $U(2N_f)$ invariant Coulomb contact interaction (34) are just the scalar product of the $U(2)_{\text{vs}}$ -vector $\vec{V}_i = (\bar{\psi}\Gamma_i\psi)$, $\Gamma_i = \{\mathbb{I}_4, \gamma^3, i\gamma^5\}$, whereas $\bar{\psi}\gamma^{35}\psi$ is a scalar. Taking into account eqs. (31), (34) and

(35) leads to the following effective low-energy four-fermion Lagrangian

$$L = \bar{\psi}i\tilde{\not{\partial}}\psi + \frac{G'_1 v_F}{2N_f} [(\bar{\psi}\psi)^2 + (\bar{\psi}\gamma^{35}\psi)^2] + \frac{G'_2 v_F}{2N_f} [(\bar{\psi}\gamma^3\psi)^2 + (\bar{\psi}i\gamma^5\psi)^2], \quad (36)$$

where $\tilde{\not{\partial}} = \gamma^\mu \tilde{\partial}_\mu$, and $G'_1 = \frac{1}{4}(G_c - \tilde{G})$, $G'_2 = \frac{1}{4}(G_c + \tilde{G})$.

Clearly, the above approximation scheme does not allow a determination of the effective coupling constants G'_1, G'_2 from an underlying microscopic lattice theory, eventually including lattice vibrations. By this reason, the above four-fermion model (36) can be only considered as a schematic one. For the following general considerations of possible exciton condensates and related phase transitions, it turns out to be reasonable to generalize this model further by omitting from now on any symmetry constraints between coupling constants. This leads us to the following schematic low-energy model for interacting fermions on a hexagonal lattice

$$L = L_0 + L_{int} = \bar{\psi}i\tilde{\not{\partial}}\psi + \left\{ \frac{1}{2N_f} G_{1vF} (\bar{\psi}\psi)^2 + \frac{1}{2N_f} G_{2vF} (\bar{\psi}\gamma^{35}\psi)^2 + \frac{1}{2N_f} H_{1vF} (\bar{\psi}i\gamma^5\psi)^2 + \frac{1}{2N_f} H_{2vF} (\bar{\psi}\gamma^3\psi)^2 \right\}. \quad (37)$$

Note once more that $\psi(x)$ in (37) transforms as a fundamental multiplet of the flavor $U(N_f)$ group, i.e. $\psi(x) \equiv \psi^a(x)$, where $a = 1, \dots, N_f$. Moreover, each component of this multiplet is a four-component Dirac spinor. (Both, the trivial summation over flavor ($a = 1, \dots, N_f$) and the summation over spinor indices in (37) are implied.) An extended four-fermion model of this type was studied in papers [17, 32] for (2+1)D QED and QCD in external magnetic and chromomagnetic fields. However, these papers have no direct physical relation to the considered honeycomb tight-binding model, its low-energy expansion, the Fierz-transformed contact Coulomb and phonon interactions and also do not use the naturally arising chiral (Weyl) representation of the Dirac algebra. Nevertheless, we can use their methods and results to our investigation of the effective potential, the solution of gap equations and the exciton mass spectrum (see Section 3.1).

It is worth noting that the general Lagrangian (37) is invariant under spatial inversion \mathcal{P} (see eq. (19)) and discrete chiral transformations

$$\gamma^5 : \psi \rightarrow \gamma^5 \psi, \quad \bar{\psi} \rightarrow -\bar{\psi} \gamma^5; \quad \gamma^3 : \psi \rightarrow \gamma^3 \psi, \quad \bar{\psi} \rightarrow \bar{\psi} \gamma^3. \quad (38)$$

For completeness and later applications, we finally introduce external magnetic fields and the chemical potential into the Lagrangian (37).

2.3.3. External magnetic fields

Let us apply the following substitutions $\partial_0 \rightarrow (\partial_0 - i\mu)$, $\partial_k \rightarrow (\partial_k + ieA_k)$ ($k = 1, 2$) to the kinetic part L_0 in eq. (37), i.e. ⁶

$$\bar{\psi}i\tilde{\not{\partial}}\psi \rightarrow \bar{\psi} \left[i\gamma^0 (\partial_0 - i\mu + i\frac{g}{2} \mu_B \vec{\sigma} \cdot \vec{B}) + i\gamma^1 v_F (\partial_x + ieA_x) + i\gamma^2 v_F (\partial_y + ieA_y) \right] \psi, \quad (39)$$

⁶The chemical potential μ arises in the tight-binding lattice model in a natural way, if one includes in eq. (1) the next-to-nearest (in-sublattice) hoppings $\Delta H_0 = -t' \sum_{\langle\langle i,j \rangle\rangle} (\psi^A(\vec{r}_i)\psi^A(\vec{r}_j) + \psi^B(\vec{r}_i)\psi^B(\vec{r}_j))$, leading to $\mu = 3t'$. Clearly, such term violates the quasiparticle-hole symmetry.

where A_x and A_y are components of the external electromagnetic vector potential. The additional term $\sim \vec{\sigma} \cdot \vec{B}$ in eq. (39) is the Zeeman energy term, which describes the (nonrelativistic) interaction of the real spin of quasiparticles with the magnetic field \vec{B} and has to be added separately. Here g is the spectroscopic Landé factor, and $\mu_B = e/(2m)$ is the Bohr magneton.

Let us now consider a tilted magnetic field $\vec{B} = (B_{\parallel}, 0, B_{\perp})$ with in-plane component B_{\parallel} in x -direction and transversal component B_{\perp} in the z -direction, transversal to the plane. (Phase transitions in planar systems under the influence of a tilted magnetic field and Zeeman interaction were recently considered in eq. [16].) It is convenient to choose a gauge, where the three-dimensional vector potential takes the form $\vec{A} = (0, \mathcal{A}_2 + B_{\perp}x, B_{\parallel}y)$ with constant \mathcal{A}_2 , so that indeed $\vec{B} = \text{rot } \vec{A}$. Obviously, the transversal component B_{\perp} couples with the orbital angular momentum L_z and spin component $\frac{1}{2}\sigma_z$, whereas the parallel component B_{\parallel} couples only to the spin of quasiparticles. Note that we admitted also a constant gauge field component \mathcal{A}_2 for later use, when we shall compactify the y -coordinate to get a nanotube cylinder. In such a case, a constant field component in the covariant derivative of the compactified direction cannot be gauged away. In particular, \mathcal{A}_2 turns out to play an important role for the description of the Aharonov-Bohm (AB) effect in hexagonal lattice nanotubes (see Sect. 4).

As is well known, the transversal field B_{\perp} leads to Landau levels of fermions and the very interesting quantum Hall effect (for details, see, e.g., ref. [49]). In the present paper, we shall, however, take $B_{\perp} = 0$ and discuss the fermionic gap equations and exciton masses in the general schematic model (37). Moreover, for illustrations and nontrivial application, we shall consider later on the simple Gross-Neveu (GN) version of the Lagrangian (37) with $G_1 \neq 0, G_2 = H_1 = H_2 = 0$, and investigate phase transitions in nanotubes in dependence on the AB-field \mathcal{A}_2 , the Zeeman interaction with \vec{B} chosen parallel to the cylinder axis and taking a finite chemical potential μ and temperature T (see Sect. 4).⁷

2.4. Exciton fields, gap equations and symmetry breaking

Let us now rewrite the Lagrangian (37) by introducing (auxiliary) excitonic fields $\sigma_1, \sigma_2, \varphi_1$, and φ_2 via the Hubbard-Stratonovich transformation

$$\mathcal{L}[\bar{\psi}, \psi, \sigma_i, \varphi_i] = \bar{\psi} \left[i\tilde{\not{D}} - \sigma_1 - \sigma_2 \gamma^{35} - \varphi_1 i\gamma^5 - \varphi_2 \gamma^3 \right] \psi - N_f \sum_{k=1}^2 \left(\frac{\sigma_k^2}{4v_F G_k} + \frac{\varphi_k^2}{4v_F H_k} \right). \quad (40)$$

Obviously, by inserting the field equations for excitonic fields

$$\sigma_1 = -2 \frac{G_1 v_F}{N_f} \bar{\psi} \psi, \quad \sigma_2 = -2 \frac{G_2 v_F}{N_f} \bar{\psi} \gamma^{35} \psi, \quad \varphi_1 = -2 \frac{H_1 v_F}{N_f} \bar{\psi} i\gamma^5 \psi, \quad \varphi_2 = -2 \frac{H_2 v_F}{N_f} \bar{\psi} \gamma^3 \psi \quad (41)$$

back into expression (40), we reproduce the Lagrangian (37).

⁷Phase transitions in (2+1)-dimensional GN-models including magnetic fields have also been studied in numerous earlier papers [13, 14, 50, 51, 52].

In order to get the Hartree-Fock gap equations for dynamical fermion masses in terms of exciton or fermion condensates, we shall take the vacuum (ground state) expectation values $\langle \dots \rangle$ on both sides of the expressions in eq. (41). This leads us to the gap equations

$$\langle \sigma_1 \rangle = -2 \frac{G_{1\nu\text{F}}}{N_f} \langle \bar{\psi} \psi \rangle = 2 \frac{G_{1\nu\text{F}}}{N_f} \text{Tr}_{sf} [iG(x, x)], \quad (42)$$

$$\langle \sigma_2 \rangle = -2 \frac{G_{2\nu\text{F}}}{N_f} \langle \bar{\psi} \gamma^{35} \psi \rangle = 2 \frac{G_{2\nu\text{F}}}{N_f} \text{Tr}_{sf} [\gamma^{35} iG(x, x)], \quad (43)$$

$$\langle \varphi_1 \rangle = -2 \frac{H_{1\nu\text{F}}}{N_f} \langle \bar{\psi} i \gamma^5 \psi \rangle = 2 \frac{H_{1\nu\text{F}}}{N_f} \text{Tr}_{sf} [i \gamma^5 iG(x, x)], \quad (44)$$

$$\langle \varphi_2 \rangle = -2 \frac{H_{2\nu\text{F}}}{N_f} \langle \bar{\psi} \gamma^3 \psi \rangle = 2 \frac{H_{2\nu\text{F}}}{N_f} \text{Tr}_{sf} [\gamma^3 iG(x, x)], \quad (45)$$

where $G(x, y)$ ($x = (x^0, \vec{r})$) is the full quasiparticle propagator which is proportional to the unit matrix in the N_f -dimensional flavor space as well as a 4×4 matrix acting in the 4-dimensional spinor space. So the symbol Tr_{sf} in eqs. (42)-(45) means the trace of an operator just over the spinor (s) and flavor (f) spaces. The inverse propagator with excitonic condensates $G^{-1}(x, x')$ has the following matrix elements in the direct product of the flavor ($a, b = 1, \dots, N_f$) and spinor spaces ($\alpha, \beta = 1, \dots, 4$)

$$[G^{-1}(x, x')]_{\alpha\beta}^{ab} = \left[i\vec{\theta} - \langle \sigma_1 \rangle - \langle \sigma_2 \rangle \gamma^{35} - \langle \varphi_1 \rangle i \gamma^5 - \langle \varphi_2 \rangle \gamma^3 \right]_{\alpha\beta} \delta^{ab} \delta^{(3)}(x - x'), \quad (46)$$

where $i\vec{\theta} = \gamma^0 i \partial_0 + i v_F \vec{\gamma} \cdot \vec{\nabla}$. It is clear that each trace over the flavor space in eqs. (42)-(45) gives there the factor N_f . Due to this reason, the solutions of the gap equations (42)-(45), i.e. the condensates $\langle \sigma_1 \rangle, \langle \sigma_2 \rangle$ etc., do not depend on N_f .

Let us finally quote the symmetry breaking properties of the condensates concerning chiral $U(2N_f)$ transformations and discrete $\mathcal{P}, C, \mathcal{T}, \gamma^5$ and γ^3 transformations (see Table 1) [7]:

(i) $\langle \bar{\psi} \psi \rangle$ – it breaks $U(2N_f)$ and discrete γ^5, γ^3 transformations, but preserves $\mathcal{P}, C, \mathcal{T}$.

(ii) $\langle \bar{\psi} \gamma^{35} \psi \rangle$ – it preserves $U(2N_f)$ and C, γ^5 and γ^3 , but breaks \mathcal{P} and \mathcal{T} . The related ‘‘Haldane mass’’ $m_2 = \langle \sigma_2 \rangle / v_F^2$ is related to the parity anomaly in (2+1) dimensions [53] (see, also ref. [54]).

(iii) $\langle \bar{\psi} i \gamma^5 \psi \rangle$ – it breaks $U(2N_f)$ and discrete \mathcal{P}, C, γ^5 , but preserves \mathcal{T} and γ^3 .

(iv) $\langle \bar{\psi} \gamma^3 \psi \rangle$ – it breaks $U(2N_f)$ and γ^3 , but preserves $\mathcal{P}, C, \mathcal{T}$ and γ^5 .

Below we demonstrate (see Section 3.1.1 and, especially, Appendix B) that, depending on the values of the coupling constants, five different phases may be implemented in the framework of the model (37). One of them is a trivial one, because its ground state is characterized by zero values of all condensates $\langle \sigma_{1,2} \rangle$ and $\langle \varphi_{1,2} \rangle$ and, therefore, has a highest possible symmetry. In each of the remaining phases only one of these condensates has a nonzero value. Hence, the ground states of these nontrivial phases of the model (37) differ in their symmetry properties (see Table 1 and/or the above points (i), ..., (iv)).

Before concluding this Section, it is worth mentioning that the axial/vector interactions appearing in a general Fierz-transformed interaction term (compare eqs. (A.9)-(A.11)) may generate additional chemical potentials dynamically. Applying again the Hubbard-Stratonovich transformation and introducing axial/vector exciton fields a_μ , one

$\langle \bar{\psi} \Gamma_i \psi \rangle$	$\langle \bar{\psi} \psi \rangle$	$\langle \bar{\psi} \gamma^{35} \psi \rangle$	$\langle \bar{\psi} i \gamma^5 \psi \rangle$	$\langle \bar{\psi} \gamma^3 \psi \rangle$
\mathcal{P}	1	-1	-1	1
\mathcal{C}	1	1	-1	1
\mathcal{T}	1	-1	1	1
γ^5	-1	1	-1	1
γ^3	-1	1	1	-1

Table 1: Transformation properties of various condensates $\langle \bar{\psi} \Gamma_i \psi \rangle$, where now $\Gamma_i = \{\mathbb{1}_4, \gamma^{35}, i\gamma^5, \gamma^3\}$, under discrete \mathcal{P} , \mathcal{C} , \mathcal{T} and γ^5 , γ^3 transformations (here we consider $\mathcal{P}: (x^0, x, y) \rightarrow (x^0, -x, y)$).

gets an additional term

$$\Delta \mathcal{L} = \sum_{k=0}^3 a_\mu^k \bar{\psi} \gamma^\mu t^k \psi - N_f \sum_{k=0}^3 \frac{1}{4v_F \widetilde{G}_k} (a_\mu^k)^2 \quad (47)$$

with general coupling constants \widetilde{G}_k . Admitting nonvanishing condensates $\langle a_0^k \rangle$, which have to be determined by respective gap equations, then provides additional dynamical chemical potentials $\mu^k = i \langle a_0^k \rangle$. The investigation of the combined system of gap equations of masses and chemical potentials is planned elsewhere.

3. Effective potential: general definitions

3.1. Hexagonal lattice sheets

Let us consider the partition function of the semi-bosonized Lagrangian (40) given by the path integral

$$Z = \int D\bar{\psi} D\psi \int D\sigma_1 D\sigma_2 D\varphi_1 D\varphi_2 \exp \left\{ i \int dx^0 d^2x \mathcal{L}[\bar{\psi}, \psi, \sigma_i, \varphi_i] \right\}. \quad (48)$$

Integrating in eq. (48) over fermion fields and rewriting the resulting determinant of the Dirac operator $\hat{D}(x, y) = D(x, y) I_{N_f}$ (being the inverse propagator given by eq. (2.46)) as $\text{Det}(\hat{D}) = (\text{Det } D)^{N_f} = \exp(N_f \text{Tr}_{sx} \ln D)$, one obtains

$$\begin{aligned} Z &= \int D\sigma_1 D\sigma_2 D\varphi_1 D\varphi_2 \exp \{ i N_f S_{\text{eff}}(\sigma_i, \varphi_i) \}, \\ S_{\text{eff}}(\sigma_i, \varphi_i) &= - \int dx^0 d^2x \sum_{k=1}^2 \left(\frac{\sigma_k^2}{4v_F G_k} + \frac{\varphi_k^2}{4v_F H_k} \right) \\ &\quad - i \text{Tr}_{sx} \ln(i\bar{\not{D}} - \sigma_1 - \sigma_2 \gamma^{35} - \varphi_1 i \gamma^5 - \varphi_2 \gamma^3). \end{aligned} \quad (49)$$

Here the quantity $S_{\text{eff}}(\sigma_i, \varphi_i)$ (49) is the effective action of the model and the Tr_{sx} -operation stands for the trace in four-dimensional spinor (s) and (2+1)-dimensional coordinate (x) spaces, respectively. Note that the expression (49) for S_{eff} can be used in order to generate one-particle irreducible Green functions of the exciton fields $\sigma_i(x)$ and $\varphi_i(x)$ in the leading order of the large- N_f expansion [15]. Moreover, the effective potential of the model is obtained by taking the effective action S_{eff} in the path integral (49) at the saddle point $\sigma_i, \varphi_i = \text{const}$,

$$V_{\text{eff}}(\sigma_i, \varphi_i) \int dx^0 d^2x = -S_{\text{eff}}(\sigma_i, \varphi_i) \Big|_{\sigma_i, \varphi_i = \text{const}}. \quad (50)$$

Following the technique of e.g. the paper [55], it is possible to find from eqs. (49) and (50) that

$$V_{\text{eff}}(\sigma_i, \varphi_i) = \sum_{k=1}^2 \left(\frac{\sigma_k^2}{4v_F G_k} + \frac{\varphi_k^2}{4v_F H_k} \right) + i \int \frac{dp_0 d^2 \vec{p}}{(2\pi)^3} \text{Tr}_s \ln D(p), \quad (51)$$

where $D(p) = p_0 \gamma^0 - v_F \vec{p} \vec{\gamma} - \sigma_1 - \sigma_2 \gamma^3 - \varphi_1 i \gamma^5 - \varphi_2 \gamma^3$ is the Fourier transformation of the flavor-independent part $D(x, y)$ of the above Dirac operator. Since $\text{Tr}_s \ln D(p) = \ln \text{Det} D(p) = \sum_i \ln \epsilon_i$, where ϵ_i are the four eigenvalues of the 4×4 matrix $D(p)$,

$$\epsilon_{1,2,3,4} = \sigma_1 \pm \sqrt{\left(\sigma_2 \pm \sqrt{p_0^2 - v_F^2 \vec{p}^2} \right)^2 - \varphi_1^2 - \varphi_2^2}, \quad (52)$$

we have from eq. (51)

$$V_{\text{eff}}(\sigma_i, \varphi_i) = \sum_{k=1}^2 \left\{ \frac{\sigma_k^2}{4v_F G_k} + \frac{\varphi_k^2}{4v_F H_k} + i \int \frac{dp_0 d^2 \vec{p}}{(2\pi)^3} \ln \left(p_0^2 - v_F^2 \vec{p}^2 - M_k^2 \right) \right\}, \quad (53)$$

where $M_{1,2} = |\sigma_2 \pm \rho|$, $\rho = \sqrt{\sigma_1^2 + \varphi_1^2 + \varphi_2^2}$. Integration over p_0 in eq. (53) can now be performed by using the general relation $\int dp_0 \ln(p_0 - A) = i\pi|A|$, which is true up to an infinite term independent of the real quantity A . So we have from eq. (53)

$$V_{\text{eff}}(\sigma_i, \varphi_i) = \sum_{k=1}^2 \left\{ \frac{\sigma_k^2}{4v_F G_k} + \frac{\varphi_k^2}{4v_F H_k} - \int \frac{d^2 \vec{p}}{(2\pi)^2} \sqrt{v_F^2 \vec{p}^2 + M_k^2} \right\}. \quad (54)$$

Since the integral term in this formula is an ultraviolet divergent improper integral, the effective potential $V_{\text{eff}}(\sigma_i, \varphi_i)$ is an ultraviolet divergent quantity. One way to obtain from eq. (54) a finite expression for the effective potential is to regularize it by simply integrating in eq. (54) over the cutted region, $|\vec{p}| < \Lambda$, in polar coordinates, where the cutoff parameter $\Lambda = O(1/a)$ is of the order of the inverse lattice spacing. As a result, we have for the regularized effective potential

$$V_{\text{eff}}(\sigma_i, \varphi_i) = \sum_{k=1}^2 \left\{ \frac{\sigma_k^2}{4v_F} \left(\frac{1}{G_k} - \frac{2\Lambda}{\pi} \right) + \frac{\varphi_k^2}{4v_F} \left(\frac{1}{H_k} - \frac{2\Lambda}{\pi} \right) + \frac{M_k^3}{6\pi v_F^2} + M_k^3 / v_F^3 O\left(\frac{M_k}{\Lambda}\right) \right\}. \quad (55)$$

In eq. (55) we have omitted constant terms, which do not depend on the dynamical parameters M_k . It is well known that coordinates of the global minimum point of the effective potential supply us with condensates $\langle \sigma_1 \rangle$, etc., as well as with a phase structure of the model. In order to simplify the investigation of the function (55) on the global minimum point, we now suppose that $M_k / \Lambda \ll 1$. In this case the last term in eq. (55) can also be omitted and $V_{\text{eff}}(\sigma_i, \varphi_i)$ takes the form

$$V_{\text{eff}}(\sigma_i, \varphi_i) = \sum_{k=1}^2 \left\{ \frac{g_k \sigma_k^2}{4v_F} + \frac{h_k \varphi_k^2}{4v_F} + \frac{M_k^3}{6\pi v_F^2} \right\}, \quad (56)$$

where we have used the notations

$$g_k = \frac{1}{G_k} - \frac{1}{G_c}, \quad h_k = \frac{1}{H_k} - \frac{1}{H_c} \quad (57)$$

and $G_c^{-1} = H_c^{-1} = \frac{2\Lambda}{\pi}$. Assuming that G_k, H_k and Λ are effective finite quantities, with Λ restricting the low-energy region of applicability, one can use for the effective potential just the finite expression (56). As a result, we see that in this case both the phase structure of the model and the condensates $\langle\sigma_1\rangle$, etc. are described (instead of the bare quantities G_k, H_k and the cutoff Λ) in terms of the finite quantities g_k and h_k .

There is yet another way to get a finite effective potential from the formally divergent expression (54). It is based on the fact that (2+1)-dimensional quantum field theories with four-fermion interactions are renormalizable in the framework of the large- N_f expansion technique [15]. So, following, e.g., the procedure of refs. [17, 32], one can renormalize the quantity (54) by introducing the cutoff parameter Λ , the renormalization scale m and renormalized coupling constants $g_k(m), h_k(m)$. It turns out that in this case the finite renormalized expression for $V_{\text{eff}}(\sigma_i, \varphi_i)$ looks like the effective potential in eqs. (56)-(57), in which the relations

$$g_k = \frac{1}{g_k(m)} - \frac{2m}{\pi}, \quad h_k = \frac{1}{h_k(m)} - \frac{2m}{\pi} \quad (58)$$

are valid also in addition to eq. (57). It is clear from eqs. (57)-(58) that in this case the parameters g_k and h_k are independent of both the renormalization scale m and the cutoff parameter Λ , i.e. they are finite and renormalization invariant parameters. As a result, the obtained renormalized effective potential (56) is also a renormalization group invariant quantity.

3.1.1. Gap equations and fermion masses

It is clear from the expression (46) for the fermion quasiparticle propagator that there might exist several dynamical fermion masses, $m_i = \langle\sigma_i\rangle/v_F^2$ or $m'_i = \langle\varphi_i\rangle/v_F^2$. (The relation between dynamical masses and energy gap in graphene-like condensed-matter systems and nanotubes is discussed, e.g. in ref. [54].) Since the excitonic condensates $\langle\sigma_i\rangle$ and $\langle\varphi_i\rangle$ are determined by the global minimum point $(\sigma_i^0, \varphi_i^0)$ of the effective potential (56), it is necessary to study its stationarity (gap) equations

$$\frac{\partial V_{\text{eff}}(\sigma_i, \varphi_i)}{\partial \sigma_i} = 0, \quad \frac{\partial V_{\text{eff}}(\sigma_i, \varphi_i)}{\partial \varphi_i} = 0, \quad i = 1, 2 \quad (59)$$

in order to find dynamical masses m_i, m'_i of fermion quasiparticles. (Note that in general the system of the gap equations (42)-(45) is equivalent to the stationarity equations (59).) The global minimum point $(\sigma_i^0, \varphi_i^0)$ of the effective potential (56) determines just the condensate values, i.e. $\sigma_i^0 = \langle\sigma_i\rangle, \varphi_i^0 = \langle\varphi_i\rangle$. (For a detailed discussion of possible condensates, dynamical fermion masses and related phase structure in dependence on general choices of coupling constants g_i, h_i we refer to refs. [17, 32] and also to Appendix B. There the extremum properties of the effective potential (56) are investigated in the most general case, i.e. for arbitrary relations between coupling constants).

For illustrations, let us specify for a moment to the $U(2) \times U(N_f)$ -symmetric model with $g_1 = g_2 = h_1 = h_2 \equiv g$. As is easily seen from eq. (57), in this particular case we have $G_i = H_i \equiv G$ ($i = 1, 2$). Moreover, in this symmetric case V_{eff} (56) simplifies to

$$V_{\text{eff}}(\sigma_i, \varphi_i) = \frac{g}{4v_F} \cdot \frac{M_1^2 + M_2^2}{2} + \frac{M_1^3}{6\pi v_F^2} + \frac{M_2^3}{6\pi v_F^2}, \quad (60)$$

where $M_{1,2}$ are given just after the expression (53). In addition, it is clear from eq. (60) that in this specific case the effective potential depends on the $O(3)$ -invariant $\rho = \sqrt{\sigma_1^2 + \varphi_1^2 + \varphi_2^2}$. So, to find the minimum value of the function $V_{\text{eff}}(\sigma_i, \varphi_i)$, it is sufficient to restrict ourselves to the configuration of the variables with, e.g., $\varphi_1 = \varphi_2 = 0, \rho = \sigma_1$. The stationarity (gap) equations for the effective potential (60) with respect to the independent variables $M_{1,2} = |\sigma_2 \pm \sigma_1|$ then read

$$\frac{\partial V_{\text{eff}}}{\partial M_i} = M_i \left(\frac{g}{4v_F} + \frac{M_i}{2\pi v_F^2} \right) = 0, \quad i = 1, 2. \quad (61)$$

It is evident from eq. (61) that for subcritical values of the bare coupling constant $G < G_c$ or, equivalently, at $g > 0$ the gap equations (61) have only a trivial solution, $M_{1,2} = 0$. It corresponds to the symmetrical global minimum point of the effective potential (60), $\langle \sigma_i \rangle = \langle \varphi_i \rangle = 0$. However, for the supercritical values of the bare coupling constant $G > G_c$ or, equivalently, at $g < 0$, the obvious solution of the gap equations (61) is $M_1 = M_2 = -\pi g v_F / 2$. Thus, expressed in terms of the variables $\sigma_{1,2}$ at $\varphi_{1,2} = 0$, in this case there are two different global minimum points of the effective potential (60) corresponding to (i) $\langle \sigma_1 \rangle = -\pi g v_F / 2, \langle \sigma_2 \rangle = \langle \varphi_1 \rangle = \langle \varphi_2 \rangle = 0$ and (ii) $\langle \sigma_2 \rangle = -\pi g v_F / 2, \langle \sigma_1 \rangle = \langle \varphi_1 \rangle = \langle \varphi_2 \rangle = 0$, i.e. the minimum value of the effective potential is degenerated. Note also that in a similar way the smallest value of the function (60) can be investigated equivalently in terms of other two variable configurations, $\sigma_1 = \varphi_2 = 0, \rho = \varphi_1$ and $\varphi_1 = \sigma_1 = 0, \rho = \varphi_2$. As a result, one can easily find that in addition to global minimum points of $V_{\text{eff}}(\sigma_i, \varphi_i)$ corresponding to the two above mentioned condensate structures (i) and (ii), there are two another global minimum points corresponding to (iii) $\langle \varphi_1 \rangle = -\pi g v_F / 2, \langle \sigma_1 \rangle = \langle \sigma_2 \rangle = \langle \varphi_2 \rangle = 0$ and (iv) $\langle \varphi_2 \rangle = -\pi g v_F / 2, \langle \sigma_1 \rangle = \langle \sigma_2 \rangle = \langle \varphi_1 \rangle = 0$. It is evident that all global minimum points, corresponding to condensate structures (i), . . . , (iv), are degenerated. However, they correspond to ground states of different phases of the model. Their symmetry properties are described in Table 1 and just after it.

3.1.2. Exciton spectrum

It is further instructive to exhibit also the mass spectrum of bound-state excitons. Suppose that the ground state of the system described by the Lagrangians (37) and (40) is determined by condensate values $\langle \sigma_k \rangle, \langle \varphi_k \rangle$ ($k = 1, 2$). To find the masses of excitons in this ground state, one should perform in the effective action $S_{\text{eff}}(\sigma_i, \varphi_i)$ of eq. (49) a shift around condensates (mean field values), $\sigma_k(x) \rightarrow \langle \sigma_k \rangle + \sigma_k(x), \varphi_k(x) \rightarrow \langle \varphi_k \rangle + \varphi_k(x)$ ($k = 1, 2$), where the quantities $\sigma_k(x), \varphi_k(x)$ are now fluctuating fields. Then it is necessary to take into account the fact that the obtained effective action $S_{\text{eff}}(\sigma_i, \varphi_i)$ is a generating functional of one-particle irreducible (1PI) Green functions of the fluctuating fields.

To be more specific, let us here consider the phase with $\langle \sigma_1 \rangle \equiv m_1 v_F^2 \sim \langle \bar{\psi} \psi \rangle \neq 0, \langle \sigma_2 \rangle = \langle \varphi_1 \rangle = \langle \varphi_2 \rangle = 0$. For the particular case $G_k = H_k = G$ ($k = 1, 2$), considered in the previous section 3.1.1, this phase corresponds to a global minimum point (i) of the effective potential (60). However, this phase is also realized for other, not so trivial as in the section 3.1.1, relations between coupling constants of the model (37), (40) [17, 32]. (See also Appendix B for the structure of the condensates in the most general case. In particular, it follows from Table B.2 that $\langle \sigma_1 \rangle = -\pi g_1 v_F / 2$.) Performing in this case a simplest field shift in the effective action (49), $\sigma_1(x) \rightarrow \langle \sigma_1 \rangle + \sigma_1(x)$, we obtain the two

point 1PI Green functions (inverse propagators) of the fluctuating fields,

$$\Gamma_{\phi_k\phi_k}(x-y) = \frac{\delta^2 S_{\text{eff}}}{\delta\phi_k(x)\delta\phi_k(y)} \Big|_{\sigma_i, \varphi_i=0}, \quad \phi_k = \{\sigma_1, \sigma_2, \varphi_1, \varphi_2\}. \quad (62)$$

It then follows from eqs. (49) and (62) that

$$\Gamma_{\phi_k\phi_k}(x-y) = -\frac{1}{2v_F G_{\phi_k}} \delta^{(3)}(x-y) + i\text{Tr}_s [\hat{t}_k G_0(x-y) \hat{t}_k G_0(y-x)], \quad (63)$$

where we use the notations

$$G_{\phi_k} = \{G_1, G_2, H_1, H_2\}, \quad \hat{t}_k = \{\mathbb{1}_4, \gamma^{35}, i\gamma^5, \gamma^3\}, \quad k = 1, \dots, 4,$$

and $G_0(x-y)$ is the inverse of the operator $(i\tilde{\partial} - \langle\sigma_1\rangle)$ with no flavor indices (recall that its mass term is $\langle\sigma_1\rangle = -\pi g_1 v_F/2 \equiv m_1 v_F^2$). It has in the spinor space the following matrix elements

$$G_0(x-y)_{\alpha\beta} = \int \frac{d^3 p}{(2\pi)^3} \left(\frac{1}{\tilde{p} - m_1 v_F^2} \right)_{\alpha\beta} e^{-ip(x-y)}, \quad (64)$$

where $\tilde{p} = (p^0, v_F \vec{p})$, and for spinor indices we have $\alpha, \beta = 1, \dots, 4$. The straightforward loop calculations, required by eq(3.16), can be found in Appendix C. In momentum space (Minkowski metric), we then obtain

$$\begin{aligned} \Gamma_{\sigma_1\sigma_1}(p) &= \frac{\tilde{p}^2 - (2m_1 v_F^2)^2}{2\pi v_F^2 \sqrt{-\tilde{p}^2}} \Gamma(p), & \Gamma(p) &= \tan^{-1} \left(\frac{\sqrt{-\tilde{p}^2}}{2m_1 v_F^2} \right), \\ \Gamma_{\sigma_2\sigma_2}(p) &= -\frac{1}{2v_F} (g_2 - g_1) + \frac{\tilde{p}^2 - (2m_1 v_F^2)^2}{2\pi v_F^2 \sqrt{-\tilde{p}^2}} \Gamma(p), & \Gamma_{\varphi_k\varphi_k}(p) &= -\frac{1}{2v_F} (h_k - g_1) - \frac{\sqrt{-\tilde{p}^2}}{2\pi v_F^2} \Gamma(p). \end{aligned} \quad (65)$$

To obtain these expressions, the gap equations (59) and the relations (57) between bare couplings G_i , H_i and finite parameters g_i , h_i have been used. It is worth emphasizing that in the case $v_F = c = 1$ our graphen-like expressions in eq. (65) coincide with the QED results obtained in refs. [15,17].

The inverse expressions of eq. (65) are just the exciton propagators, the singularities of which determine their mass spectrum and dispersion laws, i.e. the relations between their energies and spatial momenta. Thus, the scalar excitation σ_1 corresponds to a stable particle with a mass $m_\sigma = 2m_1$. The quasiparticle σ_2 is a scalar resonance, corresponding to a pole of the propagator on the second sheet of its region of analyticity. The fields φ_1 , φ_2 correspond to two scalar and pseudoscalar stable bound states of two fermions (see eq. (41) and Table 1) with nonzero binding energy. To obtain the 1PI two-point Green functions in the phase, where only $\langle\sigma_2\rangle \sim \langle\bar{\psi}\gamma^{35}\psi\rangle \neq 0$, it is required to make the replacements $\sigma_1 \leftrightarrow \sigma_2$, $g_1 \leftrightarrow g_2$ in eq. (65) etc.

It is evident that under certain restrictions of coupling constants, the considered model Lagrangian (37) acquires additional continuous symmetries. For illustrations, let us consider the effective potential (56) and assume there the condition $\{g_1 = h_1 = g < 0, g_2, h_2 > g\}$, where the global minimum point of V_{eff} corresponds to $\langle\sigma_1\rangle \sim \langle\bar{\psi}\psi\rangle \neq 0$, $\langle\sigma_2\rangle = \langle\varphi_1\rangle = \langle\varphi_2\rangle = 0$ (see Appendix B). In this case the Lagrangian (37) is invariant under continuous chiral transformations

$$U_{\gamma^5}(1) : \psi \rightarrow \exp(i\alpha\gamma^5)\psi, \quad (66)$$

where

$$\begin{aligned}
(\bar{\psi}\psi) &\rightarrow (\bar{\psi}\psi) \cos 2\alpha + (\bar{\psi}i\gamma^5\psi) \sin 2\alpha, & (\bar{\psi}i\gamma^5\psi) &\rightarrow -(\bar{\psi}\psi) \sin 2\alpha + (\bar{\psi}i\gamma^5\psi) \cos 2\alpha, \\
(\bar{\psi}\gamma^3\psi) &\rightarrow (\bar{\psi}\gamma^3\psi), & (\bar{\psi}\gamma^{35}\psi) &\rightarrow (\bar{\psi}\gamma^{35}\psi).
\end{aligned} \tag{67}$$

It then follows from eq. (65) that the propagator of the pseudoscalar field φ_1 has a pole at $\tilde{p}^2 = 0$, i.e. in the mean field (large N_f) approximation spontaneous breakdown (SB) of chiral symmetry with an associated massless Goldstone boson (GB) occurs. An analogous situation happens in the case $g_1 = h_2$ for a continuous transformation with γ^3 -generator. Note that the above discussion of SB of a continuous symmetry with associated appearance of a GB was based on the mean field approximation neglecting finite $1/N_f$ corrections. On the other hand, for finite temperature, there exists the important Mermin-Wagner-Coleman (MWC) no-go theorem [56] which for (2+1)-dimensional systems forbids SB of a continuous symmetry. In principle, this requires to go beyond the dominant expressions in the $1/N_f$ expansion and to take into account phase fluctuations of bound-state fields, related to vortex excitations and the Kosterlitz-Thouless transition [15, 57]. The consideration of related $1/N_f$ corrections is, however, outside the scope of this paper. By this reason, our numerical investigations of phase transitions at finite T and μ in Section 4 will be restricted to a simpler GN-type interaction with discrete chiral symmetry γ^5 , where the MWC-theorem does not hold.

3.2. Nanotubes from hexagonal lattice

3.2.1. Boundary conditions

For possible applications to nanotubes in magnetic fields, we shall now investigate the case where one spatial direction is compactified and the (hexagonal lattice) sheet is rolled up to a cylinder. In particular, we shall consider the cylinder as a sort of a (2+1)D brane embedded in flat (3+1)D space-time. Fermions living in the brane are then moving under the influence of a parallel homogeneous magnetic field directed along the cylinder axis. Here and in what follows we use, in the bulk, either Cartesian or cylindrical coordinates (x, y, z) or (ρ, φ, z) , respectively, and coordinates (x^1, x^2) on the cylinder surface with x^1 pointing in the z -direction, and $x^2 = R\varphi$ being the compactified coordinate, which has a length $L = 2\pi R$ with R as the cylinder radius. The basis vectors on the cylinder surface are $\mathbf{e}_1 \equiv \mathbf{e}_z$ and $\mathbf{e}_2 \equiv \mathbf{e}_\varphi$. The z -axis in the bulk is parallel to the cylinder axis, and the vector potential associated to a magnetic field B_0 parallel to the cylinder (z)-axis is given by $\vec{A} = \frac{e}{2}B_0\mathbf{e}_\varphi$ in the bulk and as $\vec{\mathcal{A}} = \frac{R}{2}B_0\mathbf{e}_\varphi$ on the cylinder surface. This field $\vec{\mathcal{A}}$ has to be included in the form of a covariant derivative by replacing $\partial_2 \rightarrow D_2 = \partial_2 + ie\mathcal{A}_2$ in the Lagrangian. Alternatively, one might also keep ∂_2 and include an effective magnetic phase ϕ ,

$$\phi = \frac{e\mathcal{A}_2L}{2\pi} = \frac{\Phi_m}{\Phi_m^0} \tag{68}$$

into the boundary condition of the fermion field $\psi(x^0, x^1, x^2)$

$$\psi(x^0, x^1, x^2 + L) = e^{2\pi i(\phi + \alpha)} \psi(x^0, x^1, x^2). \tag{69}$$

Here Φ_m is the magnetic flux passing through the tube cross section, $\Phi_m^0 = 2\pi/e$ is the magnetic flux quantum and α is determined by the lattice structure (cf. eq. (70)). Notice that the above type of interaction with a magnetic flux Φ

inserted via \mathcal{A}_2 in the covariant derivative D_2 can just be considered as a manifestation of the Aharonov-Bohm (AB) effect [39]. At the same time, an external bulk magnetic field B_{\parallel} included in the direction of the cylinder axis and existing at the cylinder surface should also lead to a Zeeman spin-interaction. In fact, the magnetic moment from the real spin of fermions will interact with the surface magnetic field B_{\parallel} . Such a Zeeman term has then to be added as in eq. (39).

Taking into account the properties of the hexagonal graphene-like lattice in nanotubes, it has been shown that the fermion field $\psi(t, \vec{r})$ satisfies at the K -point the following boundary condition [39, 40]

$$\psi_K(x^0, \vec{r} + \vec{L}) = e^{2\pi i(\phi - \frac{1}{3}\nu)} \psi_K(x^0, \vec{r}), \quad (70)$$

where $\nu = (0, \pm 1)$, and the phase ϕ is given in eq. (68). An analogous expression follows for $\psi_{K'}$ with the replacement $\nu \rightarrow -\nu$,

$$\psi_{K'}(x^0, \vec{r} + \vec{L}) = e^{2\pi i(\phi + \frac{1}{3}\nu)} \psi_{K'}(x^0, \vec{r}). \quad (71)$$

The field spinors satisfying the boundary conditions (70), (71) can be written as Fourier decomposition

$$\psi = \begin{pmatrix} \psi_K^A \\ \psi_K^B \\ -i\psi_{K'}^B \\ i\psi_{K'}^A \end{pmatrix} = \frac{1}{L} \sum_{n=-\infty}^{\infty} e^{i\left[\frac{2}{R}(n+\phi) + p_1 x^1 + p_0 x^0\right]} \begin{pmatrix} \psi_{Kn}^{(1)} \\ \psi_{K'n}^{(2)} \end{pmatrix}, \quad (72)$$

where

$$\begin{aligned} \psi_{Kn}^{(1)} &= \begin{pmatrix} \psi_{Kn}^A \\ \psi_{Kn}^B \end{pmatrix} e^{-i\frac{2}{R}\left(\frac{\nu}{3}\right)} \\ \psi_{K'n}^{(2)} &= \begin{pmatrix} -i\psi_{K'n}^B \\ i\psi_{K'n}^A \end{pmatrix} e^{i\frac{2}{R}\left(\frac{\nu}{3}\right)}. \end{aligned} \quad (73)$$

This then leads for $\nu \neq 0$ to a nonvanishing ("semiconductor") gap $\Delta\mathcal{E}$ between the conduction and valence bands of non-interacting fermions with vanishing dynamical masses. Indeed, the azimuthal components of the p_2 momentum are

$$p_{\nu\phi}(n) = \frac{2\pi}{L}(n + \phi - \frac{\nu}{3}), \quad (74)$$

so that

$$\Delta\mathcal{E}(n = \phi = p_1 = 0) = v_F \frac{4\pi}{L} \frac{|\nu|}{3} \neq 0. \quad (75)$$

On the other hand, $\Delta\mathcal{E} = 0$ if $\nu = 0$, and one gets "metallic" behavior [39, 40]. Obviously, such an energy gap increases in the insulator phase with a dynamical mass gap m , where one has

$$\mathcal{E}^{\pm}(p_1, p_{\nu\phi}(n)) = \pm \sqrt{v_F^2 p_1^2 + v_F^2 p_{\nu\phi}^2(n) + (mv_F^2)^2}, \quad (76)$$

and thus

$$\Delta\mathcal{E}(n = p_1 = \phi = 0) = 2 \sqrt{v_F^2 \left(\frac{2\pi}{L}\right)^2 \left(\frac{\nu}{3}\right)^2 + (mv_F^2)^2}. \quad (77)$$

3.2.2. Thermodynamic potential for nanotubes

Let us finally consider the thermodynamic potential Ω_T for a nanotube at finite temperature and particle density. In this case, we have to calculate the Tr-operation in eq. (49) by taking into account the Fourier decomposition (72) of spinors. In order to get the corresponding (unrenormalized) thermodynamic potential Ω_T , one has to perform a replacement of the p_0 -integration in eq. (53) by a summation over Matsubara frequencies ω_ℓ , following the rule

$$\int_{-\infty}^{\infty} \frac{dp_0}{2\pi} f(p_0) \rightarrow \frac{i}{\beta} \sum_{\ell=-\infty}^{\infty} f(i\omega_\ell), \quad (78)$$

where $\omega_\ell = \frac{2\pi}{\beta} \left(\ell + \frac{1}{2} \right)$, $\ell = 0, \pm 1, \pm 2, \dots$ and $\beta = \frac{1}{T}$ is the inverse temperature. Next, the chemical potential μ will be introduced by the standard shift $\omega_\ell \rightarrow \omega_\ell - i\mu$ ⁸. Finally, we have to take into account the boundary condition of the nanotube which requires to replace the momentum component p_2 by the expression (74), $p_2 \rightarrow p_{v\phi}(n) = \frac{2\pi}{L} \left(n + \phi - \frac{\nu}{3} \right)$, where the phase ϕ is expressed by the magnetic AB-flux (see eq. (68)). A lengthy but straightforward calculation then gives

$$V_{\text{eff}}(\sigma_i, \varphi_i, T, \hat{\mu}, \phi) = \sum_{k=1}^2 \left\{ \left(\frac{\sigma_k^2}{4v_F G_k} + \frac{\varphi_k^2}{4v_F H_k} \right) - \frac{1}{\beta L} \sum_{s=\pm 1} \sum_{\ell=-\infty}^{\infty} \sum_{n=-\infty}^{\infty} \int \frac{dp_1}{2\pi} \ln \left[\left(\frac{2\pi}{\beta} \left(\ell + \frac{1}{2} \right) - i\hat{\mu} \right)^2 + v_F^2 \left(\frac{2\pi}{L} \right)^2 \left(n + \phi - \frac{\nu}{3} \right)^2 + v_F^2 p_1^2 + M_k^2 \right] \right\}, \quad (79)$$

where we have included the Zeeman term into the effective chemical potential μ according to eq. (39),

$$\hat{\mu} = \mu - \frac{g}{2} s \mu_B B_{\parallel} \quad (80)$$

with $s = \pm 1$ for up/down spin, and the mass gaps M_k are given after eq.(53). Eq. (79) is one of the main results of this paper.

In the next Section we shall use V_{eff} for a numerical investigation of the chiral phase transition in the (β, L) and (μ, T) plane in dependance on the magnetic flux ϕ . For a first application and as illustration, we shall restrict us now to a simple model version of eq. (79) by choosing coupling constants in such a way that the mean field solutions are $\sigma_1 = \sigma \neq 0, \sigma_2 = \varphi_1 = \varphi_2 = 0$. Neglecting temporarily the Zeeman effect, putting $\hat{\mu} \rightarrow \mu$, we then have ($G_1 \rightarrow G$)

$$V_{\text{eff}}(\sigma, T, \mu, \phi) = \frac{\sigma^2}{4v_F G} - \frac{2}{\beta L} \sum_{\ell=-\infty}^{\infty} \sum_{n=-\infty}^{\infty} \int \frac{dp_1}{2\pi} \ln \left[\left(\frac{2\pi}{\beta} \left(\ell + \frac{1}{2} \right) - i\mu \right)^2 + v_F^2 \left(\frac{2\pi}{L} \right)^2 \left(n + \phi - \frac{\nu}{3} \right)^2 + v_F^2 p_1^2 + \sigma^2 \right]. \quad (81)$$

Note that expression (81) generalizes the results of the compactified Gross–Neveu (GN) models [33, 34, 38, 40] to finite T and μ . Recall also that when investigating the thermodynamic potential (81) of the compactified GN-model, the MWC-theorem [56] does not apply, since one considers the spontaneous breakdown and restoration of a discrete chiral γ^5 -symmetry at finite T .

⁸After taking temperature and chemical potential into account, the effective potential of the model acts as a thermodynamic potential. However, in order to keep consistency in different sections of the present paper, we shall continue to denote it as V_{eff} .

4. Chiral phase transitions in nanotubes

4.1. Phase structure in nanotubes with non-zero chemical potential

As an illustration of the above general results, we will now investigate the phase transitions in the model described by eq. (81), omitting, for simplicity, the influence of the Zeeman effect and taking further $\nu = 0$ (metallic case), but considering finite temperature and chemical potential. We will, however, keep the Aharonov-Bohm phase ϕ untouched for further calculations. After subtraction of terms independent of σ that do not affect the symmetry properties, we write

$$V_{\text{eff}} = \frac{\sigma^2}{4v_{\text{F}}G} - \frac{2}{\beta L} \sum_{\ell=-\infty}^{\infty} \sum_{n=-\infty}^{\infty} \int \frac{dp_1}{2\pi} \ln \left[1 + \frac{\sigma^2}{\left(\frac{2\pi}{\beta}(\ell + \frac{1}{2}) - i\mu\right)^2 + (v_{\text{F}}\frac{2\pi}{L})^2(n + \phi)^2 + v_{\text{F}}^2 p_1^2} \right]. \quad (82)$$

Further we use the following formula:

$$\begin{aligned} \sum_{\ell=-\infty}^{\infty} \ln \left(1 + \frac{b^2}{(\ell + \alpha)^2 + a^2} \right) &= \sum_{\ell=-\infty}^{\infty} (\ln((\ell + \alpha)^2 + a^2 + b^2) - \ln((\ell + \alpha)^2 + a^2)) \\ &= \int_{-\infty}^{\infty} d\tau \ln \left(1 + \frac{b^2}{\tau^2 + a^2} \right) + \ln \frac{1 - 2 \cos(2\pi\alpha) e^{-2\pi\sqrt{a^2+b^2}} + e^{-4\pi\sqrt{a^2+b^2}}}{1 - 2 \cos(2\pi\alpha) e^{-2\pi\sqrt{a^2}} + e^{-4\pi\sqrt{a^2}}}, \end{aligned} \quad (83)$$

which can be found e.g. in eq. [33], and obtain

$$\begin{aligned} V_{\text{eff}} &= \frac{\sigma^2}{4v_{\text{F}}G} - \frac{2}{L} \sum_{n=-\infty}^{\infty} \int \frac{dp_1}{2\pi} \frac{dp_0}{2\pi} \ln \left[1 + \frac{\sigma^2}{(v_{\text{F}}\frac{2\pi}{L})^2(n + \phi)^2 + v_{\text{F}}^2 p_1^2 + p_0^2} \right] - \\ &\quad - \frac{2}{\beta L} \sum_{n=-\infty}^{\infty} \int \frac{dp_1}{2\pi} \ln \left[1 + 2 \text{ch}(\beta\mu) \exp(-\beta E_{n,p_1}) + \exp(-2\beta E_{n,p_1}) \right], \end{aligned} \quad (84)$$

where $E_{n,p_1} = \sqrt{v_{\text{F}}^2 p_1^2 + (v_{\text{F}}\frac{2\pi}{L})^2(n + \phi)^2 + \sigma^2}$. To transform the second summand in V_{eff} , we use eq. (83). The result is $V_{\text{eff}} = V_{(0)} + V_{(L)} + V_{(\mu T)}$, where

$$V_{(0)} \equiv \frac{\sigma^2}{4v_{\text{F}}G} - 2 \int \frac{d^3 p}{(2\pi)^3} \ln(p_0^2 + v_{\text{F}}^2 p_1^2 + v_{\text{F}}^2 p_2^2 + \sigma^2) = \frac{1}{\pi v_{\text{F}}^2} \left(\frac{|\sigma|^3}{3} - \frac{\sigma^2 \sigma_0}{2} \right), \quad \sigma_0 = -\pi v_{\text{F}} g / 2, \quad (85)$$

$$\begin{aligned} V_{(L)} &= -\frac{2}{L} \int \frac{d^2 p}{(2\pi)^2} \ln \frac{1 - 2 \cos(2\pi\phi) e^{-\frac{L}{v_{\text{F}}}\sqrt{p_0^2 + v_{\text{F}}^2 p_1^2 + \sigma^2}} + e^{-2\frac{L}{v_{\text{F}}}\sqrt{p_0^2 + v_{\text{F}}^2 p_1^2 + \sigma^2}}}{1 - 2 \cos(2\pi\phi) e^{-\frac{L}{v_{\text{F}}}\sqrt{p_0^2 + v_{\text{F}}^2 p_1^2}} + e^{-2\frac{L}{v_{\text{F}}}\sqrt{p_0^2 + v_{\text{F}}^2 p_1^2}}} = \\ &= \frac{2v_{\text{F}}}{\pi L^3} \sum_{n=1}^{\infty} \frac{\cos(2\pi\phi n)}{n^3} e^{-\frac{L\sigma n}{v_{\text{F}}}} + \frac{2\sigma}{\pi L^2} \sum_{n=1}^{\infty} \frac{\cos(2\pi\phi n)}{n^2} e^{-\frac{L\sigma n}{v_{\text{F}}}} = \\ &= 2\Re e \left(\frac{v_{\text{F}}}{\pi L^3} \text{Li}_3(e^{-\frac{L}{v_{\text{F}}}\sigma + 2\pi i\phi}) + \frac{\sigma}{\pi L^2} \text{Li}_2(e^{-\frac{L}{v_{\text{F}}}\sigma + 2\pi i\phi}) \right), \end{aligned} \quad (86)$$

$$\begin{aligned} V_{(\mu T)} &= -\frac{2}{\beta L} \sum_{n=-\infty}^{\infty} \int \frac{dp_1}{2\pi} \ln \left(1 + 2 \cosh(\beta\mu) \exp(-\beta E_{n,p_1}) \exp(-2\beta E_{n,p_1}) \right) \\ &= -\frac{2}{\beta L} \sum_{n=-\infty}^{\infty} \int \frac{dp_1}{2\pi} \left[\ln \left(1 + e^{-\beta(E_{n,p_1}^+)} \right) + \ln \left(1 + e^{-\beta(E_{n,p_1}^-)} \right) \right], \end{aligned} \quad (87)$$

and $E_{n,p_1}^{\pm} = E_{n,p_1} \pm \mu$. Note that the quantity $V_{(0)}$ in eq. (85) is the effective potential of the system in vacuum, i.e. at $T = 0$ and $\mu = 0$. Hence, its final expression in the right hand side of (85) can be obtained in the same way as in Sect.

3.1 (compare eq. (85) with the more general expression (56)). So, the renormalization invariant coupling constant g in eq. (85) is a particular case of relations (57), $g = 1/G - 1/G_c$. At $T = 0, \mu = 0$ and $g < 0$ the parameter σ_0 in eq. (85) is the nonzero vacuum expectation value of the σ field, $\sigma_0 = \langle \sigma(x) \rangle$, which corresponds to spontaneous breaking of γ^5 chiral symmetry. However, at $g > 0$ we have in this case $\langle \sigma(x) \rangle = 0$ and intact γ^5 symmetry. Moreover, Li_s are polylogarithms (here di- and trilogarithms), while $\Re e$ means the real part of the expression. Further numerical calculations resulted in the graphs shown below. For instance, Fig. 3 demonstrates the phase structure of the model in the plane (T, μ) with $\phi = 0.05 \approx 0$ (an actual numerical computation for $\phi = 0$ gives nearly the same result, but requires much more time for drawing accurate plots). The temperature is given in units of the critical temperature $T_c = \frac{1}{\beta_c} = \frac{\pi|g|v_F}{4 \ln(2)}$ and the chemical potential is given in units of $\mu_c = \pi|g|v_F/2$, where $g = g_1$ is defined in eq. (58). These values correspond to the temperature and chemical potential that restore symmetry in a "flat" model without any other external parameters. The circumference of the compactified dimension is chosen small enough to make the model differ from the "flat" one ($L = 1.2L_c$, where $L_c = v_F\beta_c$). The resulting structure is similar to what has been found in ref. [4] for a 2D GN model. The result can be interpreted as a manifestation of dimensional reduction in the asymmetrical phase, which exists for low enough temperature and periodic boundary conditions (see ref. [58]). Areas I and III in Fig. 3 correspond to broken symmetry. The difference between them is that in area I only one minimum of V_{eff} exists and is located at $\sigma \neq 0$, whereas in area III there are two minima. Additionally to the one presented in area I, there is a local minimum at $\sigma = 0$, and a global one at $\sigma \neq 0$. Areas II and IV are areas of restored symmetry. In area II only the trivial minimum at $\sigma = 0$ exists, while in area IV there are two local minima of the effective potential, the trivial one and a non-trivial one at $\sigma \neq 0$, however the global minimum is trivial. Hence the line BE in Fig. 3 is the line of a phase transition of the first kind, whereas the line AB is the line of a phase transition of the second kind. Lines BD and BC are not lines of phase transitions, but are lines, where the trivial and non-trivial minima vanish/appear as local minima.

Obviously, when the Zeeman effect is taken into account by the replacement $\mu \rightarrow \hat{\mu}$, only the summand $V_{(\mu T)}$ needs to be modified, leading to

$$V_{(\mu T)}^Z = -\frac{1}{\beta L} \sum_{n=-\infty}^{\infty} \int \frac{dp_1}{2\pi} \left[\ln \left(1 + e^{-\beta(E_{n,p_1})_{\uparrow}^+} \right) + \ln \left(1 + e^{-\beta(E_{n,p_1})_{\uparrow}^-} \right) + \ln \left(1 + e^{-\beta(E_{n,p_1})_{\downarrow}^+} \right) + \ln \left(1 + e^{-\beta(E_{n,p_1})_{\downarrow}^-} \right) \right], \quad (88)$$

where $(E_{n,p_1})_{\uparrow\downarrow}^{\pm} = E_{n,p_1} \pm \mu_{\uparrow\downarrow}$ and $\mu_{\uparrow\downarrow}$ represents $\hat{\mu}$ for $s = \pm 1$. Symmetry between μ and $\delta\mu = \frac{g}{2}\mu_B B_{\parallel}$ can now be noticed. In fact, the replacement $\mu \leftrightarrow \delta\mu$ does not change the effective potential. Hence Fig. 3 can also be interpreted as the phase structure of the system under the influence of the Zeeman effect but with a vanishing chemical potential.

4.2. Phase structure in nanotubes under the influence of the Aharonov–Bohm effect

Here we will investigate the influence of the Aharonov–Bohm effect on the symmetry properties of the nanotubes at zero chemical potential. From the discussion after eq. (68) it is, in particular, clear that the Aharonov–Bohm effect represents the change in the periodicity condition for the nanotubes.

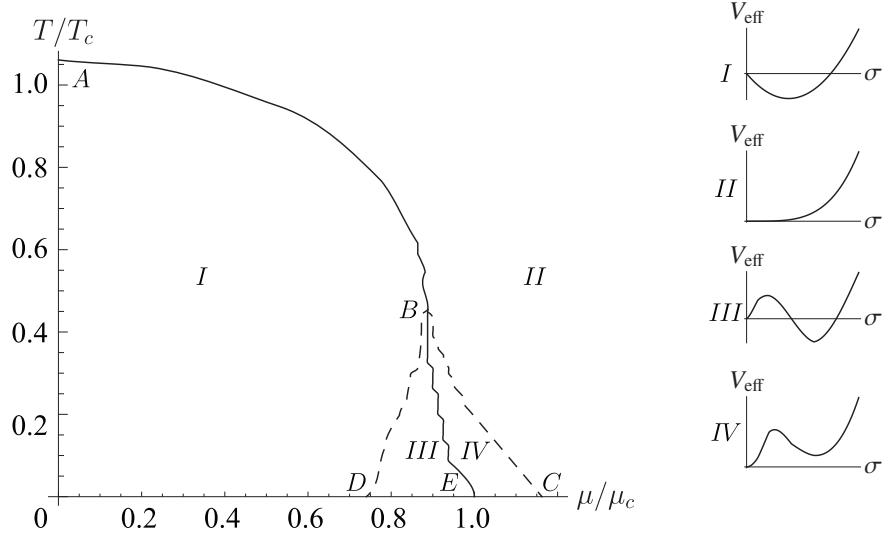


Figure 3: Phase diagram of the model under the influence of chemical potential and temperature. Figures in the right schematically show the behavior of the effective potential V_{eff} as a function of σ . The explanation of the phases I-IV is given in the text below.

Let us put $\mu = 0$ in the general formula (81) and calculate $V_{\text{eff}}(\sigma, \phi, T, \mu)|_{\mu=0}$. By using the proper time representation:

$$\ln \frac{A}{B} = - \int_0^{\infty} \frac{ds}{s} (\exp(-sA) - \exp(-sB)) \quad (89)$$

and Poisson resummation formula

$$\sum_{\ell=-\infty}^{+\infty} \exp \left[-s \left(\frac{2\pi\ell}{B} + C \right)^2 \right] = \frac{B}{2\sqrt{\pi s}} \left[1 + 2 \sum_{\ell=1}^{+\infty} \exp \left(-\frac{B^2\ell^2}{4s} \right) \cos(BC\ell) \right], \quad (90)$$

we write the effective potential in the form

$$V_{\text{eff}}(\sigma, \phi, T) = \frac{\sigma^2}{4v_F G} + \frac{1}{4\pi^{3/2} v_F^2} \int_0^{\infty} \frac{ds}{s^{5/2}} \left[\exp(-s\sigma^2) \right] \times \left[1 + 2 \sum_{\ell=1}^{+\infty} (-1)^\ell \exp \left(-\frac{\beta^2 \ell^2}{4s} \right) \right] \times \left[1 + 2 \sum_{n=1}^{+\infty} \exp \left(-\frac{L^2 n^2}{4s v_F^2} \right) \cos(2\pi n\phi) \right] + \text{c.t.}, \quad (91)$$

where the counterterm c.t. does not depend on the parameters to be investigated and is further omitted. Various combinations of products of summands in the last two factors of the above formula correspond to different physical situations. By considering only summands that are equal to unity, we can investigate a “flat” (2+1)D GN model without compactification, temperature and external fields ($L \rightarrow \infty$, $T = 0$, $\mathcal{A}_2 = 0$). The term containing $\beta = 1/T$ in the exponent of the first cofactor gives the temperature dependence, while the summand containing L in the exponent of the second cofactor is due to compactification of spatial dimension (with respect to boundary conditions). One of

the key characteristics of the GN model is the restoration of chiral symmetry ($\sigma \rightarrow 0$) under the influence of high temperature. In this section we aim at the study of the role of all the parameters (L, T, \mathcal{A}_2), while in ref. [34] this model was investigated at $T = 0$. The consideration of all the summands along with their product allows to consider now the case of finite temperature and spatial compactification at the same time. The entire effective potential is the sum of all its parts

$$V_{\text{eff}} = V_{(0)} + V_{(T)} + V_{(L)} + V_{(\times)}, \quad (92)$$

where $V_{(0)}$, $V_{(T)}$, and $V_{(L)}$ correspond to zero temperature, finite temperature and compactification parts, respectively, while the cross-term $V_{(\times)}$ describes the simultaneous role of temperature and compactification in the model.

The summand $V_{(0)}$, corresponding to the ‘‘flat’’ model, and the summand $V_{(L)}$, representing the influence of compactification, were found earlier in eqs. (85) and (86); in eq. (91) summand $V_{(0)}$ corresponds to the term which include the first summand (equal to 1) in the first square brackets and the first summand (equal to 1) in the second square brackets, while summand $V_{(L)}$ corresponds to the term which include the first summand in the first square brackets and the second summand in the second square brackets. As for summands $V_{(T)}$ and $V_{(\times)}$, which correspond to the second summand in the first square brackets of (91) and first and second summands in the second square brackets respectively, we will calculate them in a different way in order to show the symmetry between spatial compactification and usual temporal compactification just related to finite temperature.

Thermal term $V_{(T)}$, i.e. the term that contains the second summand in the first square brackets of (91) and the first summand in the second square brackets (equal to 1), can be calculated by integrating over s via the formula

$$\int_0^{\infty} x^{-n-1/2} e^{-px-q/x} dx = (-1)^n \sqrt{\frac{\pi}{p}} \frac{\partial^n}{\partial q^n} e^{-2\sqrt{pq}} \quad (93)$$

with $n = 2$ and using the definition of polylogarithm function $\text{Li}_\nu(x) = \sum_{k=1}^{\infty} \frac{x^k}{k^\nu}$. The result of this calculation is similar to that for $V_{(L)}$ in eq. (86)

$$\begin{aligned} V_{(T)} &= \frac{1}{2\pi^{3/2}v_F^2} \int_0^{\infty} \frac{ds}{s^{5/2}} [\exp(-s\sigma^2)] \times \left[2 \sum_{\ell=1}^{+\infty} (-1)^\ell \exp\left(-\frac{\beta^2 \ell^2}{4s}\right) \right] = \\ &= \frac{2}{\pi\beta^3 v_F^2} \left[\sigma\beta \text{Li}_2(-e^{-\sigma\beta}) + \text{Li}_3(-e^{-\sigma\beta}) \right]. \end{aligned} \quad (94)$$

The cross-term $V_{(\times)}$ of the effective potential cannot be expressed in terms of special functions, and we will take it

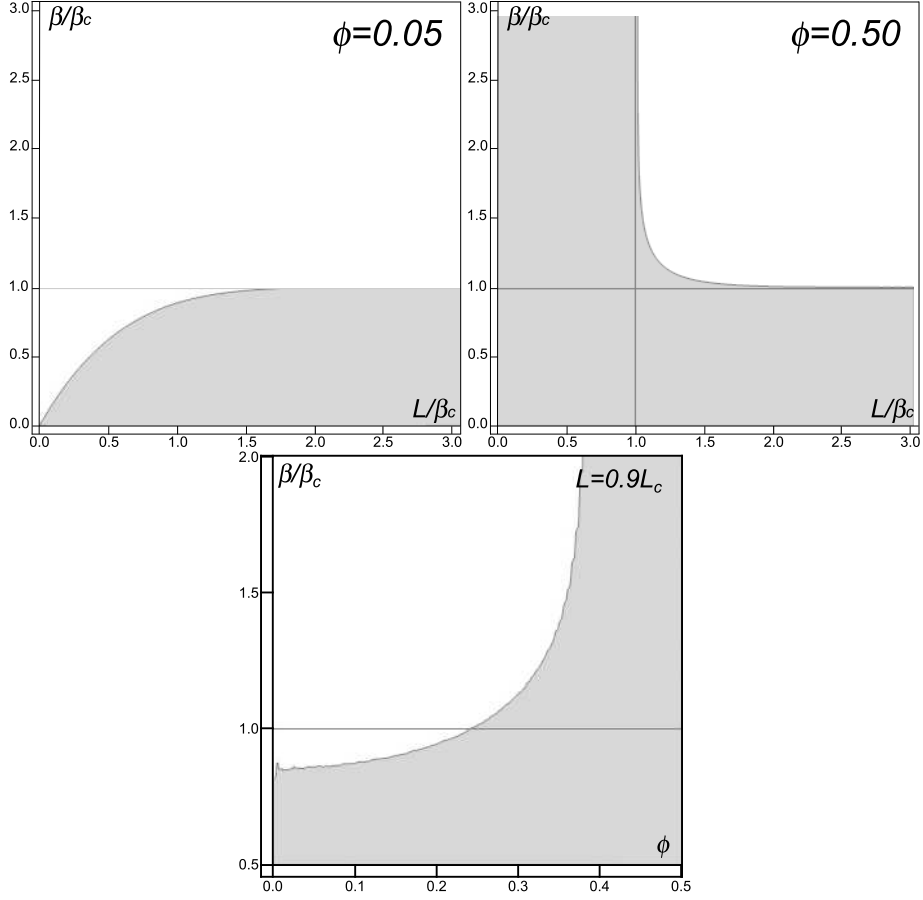


Figure 4: Phase diagrams of the model in (L, β) coordinates with different values of the magnetic phase ϕ and in the plane (ϕ, β) with fixed $L < L_c$. The painted area of graphs corresponds to the symmetrical phase, while the unpainted one corresponds to the broken symmetry.

into account by using numerical calculations

$$\begin{aligned}
 V_{(\infty)} &= \frac{1}{4\pi^{3/2}v_F^2} \int_0^\infty \frac{ds}{s^{5/2}} \left[\exp(-s\sigma^2) \right] \times \left[2 \sum_{\ell=1}^{+\infty} (-1)^\ell \exp\left(-\frac{\beta^2 \ell^2}{4s}\right) \right] \times \\
 &\quad \times \left[2 \sum_{n=1}^{+\infty} \exp\left(-\frac{L^2 n^2}{4sv_F^2}\right) \cos(2\pi n\phi) \right] = \\
 &= \frac{4}{\pi v_F^2} \sum_{\ell=1}^{+\infty} \sum_{n=1}^{+\infty} \left\{ (-1)^\ell \cos(2\pi n\phi) \left[\exp\left(-\sigma \sqrt{\beta^2 \ell^2 + \frac{L^2 n^2}{v_F^2}}\right) \times \frac{\sigma \sqrt{\beta^2 \ell^2 + \frac{L^2 n^2}{v_F^2} + 1}}{\left(\sqrt{\beta^2 \ell^2 + \frac{L^2 n^2}{v_F^2}}\right)^3} \right] \right\}.
 \end{aligned} \tag{95}$$

With the effective potential thus obtained, we can draw corresponding phase diagrams of the model. Fig. 4 shows phase diagrams in the (L, β) and (ϕ, β) coordinates. The painted area of graphs corresponds to the symmetrical phase, while the unpainted one corresponds to the broken symmetry. Note, that since the constant g is dimensional, we can multiply all dimensional parameters by proper powers of $|g|$ (if $g < 0$) to make them dimensionless in the quasi-Plank

unit system with $\hbar = c = |g| = 1$. Thus, in all the diagrams we assume that $g = -1$. Evidently, the chiral symmetry is broken in the “flat” limit, when $T \rightarrow 0, L \rightarrow \infty$. The inverse temperature β and compactification length L on the pictures are normalized by the critical values β_c and L_c introduced earlier. We have chosen $\phi = 0.05$ as value close to zero, since it can be shown that the phase diagram with $\phi \equiv 0$ is nearly the same [59]. However, to draw that diagram one should write the effective potential in a different form, in which the symmetry between L and β is not obvious. The corresponding lengthy and straightforward calculation is not included in this paper. The symmetry between the influence of finite temperature and spatial compactification mentioned above is especially evident on the graph corresponding to $\phi = 1/2$, which could be predicted from eq. (91). The reduction of the spatial circle length gives thus the same result as an increase of the temperature. It should be mentioned that symmetry breaking and dimensional reduction in a 3D GN model were discussed in ref. [58] with periodic, $\phi = 0$, and antiperiodic, $\phi = 1/2$, boundary conditions, but without taking the influence of temperature into account. We found it interesting that in the case of small ϕ spatial compactification counteracts the symmetry restoration caused by the temperature. It is also interesting that a temperature higher than the critical one in the “flat” model is necessary to restore the symmetry, if ϕ is small enough. However, the symmetry can be restored independently of the phase ϕ and compactification length L , if the temperature is high enough.

5. Summary and conclusions

In this paper we have investigated chiral symmetry breaking in (2+1)D models with four-fermion interaction that are effectively used in studying polymers, and especially graphene. In Sect. 2 we started from a “honeycomb” graphene-like lattice-based Hamiltonian (5), to which we then added the four-fermion interaction terms (31). Via Fierz transformation (see Appendix A), we then obtained Lagrangian (36) and, by omitting any symmetry relations between coupling constants, finally arrived at the generalized GN-type schematic model (37). In Sect. 3 we studied the condensates appearing in the model and found the gap equation (61) clearly demonstrating that the chiral symmetry of the model can be broken by non-zero condensates, depending on the magnitude of the coupling constant.

The symmetry properties of the appearing condensates with respect to discrete chiral and C , \mathcal{P} and \mathcal{T} transformations are then considered in Table 1. Some lengthy calculations and discussions involving the phase structure of the obtained generalized Gross–Neveu model are given in Appendix B. Moreover, in eq. (65) we have collected the 1PI two-point Green functions (inverse propagators) of exciton fields resulting from fermion loop calculations in Appendix C.

In addition, we have also investigated carbon nanotubes with corresponding boundary conditions (70) and (71) incorporating the effect of an external magnetic field. As a result, we calculated the effective thermodynamic potential for the nanotube model (81) including effects of finite temperature, particle density and external magnetic fields. As illustration, we numerically investigated in Sect. 4 the chiral symmetry properties after simplifying the model by taking into account only one condensate. In this case, the model is reduced to a standard Gross–Neveu model with

only a discrete γ^5 chiral symmetry. The phase diagram in the (μ, T) plane is drawn in Fig. 3 which shows its great similarity with the phase diagram of the 2D Gross–Neveu model presented in ref. [4].

Finally, we investigated the phase structure under the influence of the Aharonov–Bohm effect and showed that this effect can greatly influence the phase structure of the system (Fig. 4). Here we can notice that, depending on the Aharonov–Bohm phase, compactification of spatial dimension can either oppose or assist the thermal restoration of the originally broken chiral symmetry, i.e. in the case of periodical boundary conditions restoration of chiral symmetry requires a greater temperature than in the planar model. On the contrary, with an antiperiodic boundary condition (that can be provided by the Aharonov–Bohm effect), the temperature required for the symmetry restoration is lower than in the planar model. Then, if the radius of the compactified dimension is small enough, the chiral symmetry can be restored even at zero temperature.

Acknowledgments

One of the authors (D.E.) is grateful to G.W. Semenoff, H.Reinhardt, V.V. Braguta, and V.A. Miransky for useful discussions.

Appendix A. Fierz-transformed interactions

For completeness, we compile in this appendix the formulas, required to obtain the Fierz-transformed expressions of the four-fermion interaction in eqs. (34) and (35) of the text.

Let us consider the 16 Hermitian 4×4 matrices of the Dirac algebra $\{\Gamma\}_{A=1}^{16}$ quoted in eq. (32). Then, any Hermitian matrix M can be written as $M = \frac{1}{4} (\text{Tr} M \Gamma^A) \Gamma^A$, where summation over repeated indices is understood. The last expression for M can be rewritten as

$$4\delta_{\ell i} \delta_{m j} M_{\ell m} = \Gamma_{m\ell}^A \Gamma_{ij}^A M_{\ell m}, \quad (\text{A.1})$$

leading to the identity $\delta_{\ell i} \delta_{m j} = \frac{1}{4} \Gamma_{m\ell}^A \Gamma_{ij}^A$. Using this identity, one can rewrite the product of two matrix elements as

$$M_{ij} N_{mn} = \frac{1}{16} (\text{Tr} M \Gamma^A N \Gamma^B) \Gamma_{in}^B \Gamma_{mj}^A. \quad (\text{A.2})$$

This then leads to the required expansion of a four-fermion term as [29]

$$\begin{aligned} & \left[\bar{\psi}^{(a,s)}(x) M \psi^{(b,s')}(x) \right] \left[\bar{\psi}^{(c,s'')}(y) N \psi^{(d,s''')}(y) \right] (\delta^{ab} \delta^{cd}) (\delta^{ss'} \delta^{s''s'''}) \\ &= -\frac{1}{16} (\text{Tr} M \Gamma^A N \Gamma^B) \left[\bar{\psi}^{(a,s)}(x) \Gamma^B \psi^{(d,s''')}(y) \right] \left[\bar{\psi}^{(c,s'')}(y) \Gamma^A \psi^{(b,s')}(x) \right] (\delta^{ab} \delta^{cd}) (\delta^{ss'} \delta^{s''s'''}) \end{aligned} \quad (\text{A.3})$$

which is used in the text for $x = y$. The minus sign in the last line arises from the Grassmann nature of the fermion fields. In a second step, we have to Fierz-transform the spin and flavor singlet structure of the interaction terms by using the completeness relations for the spin and flavor groups $U(S)$, $U(N)$,

$$\frac{1}{2} \delta^{s's'} \delta^{s''s'''} = \frac{1}{4} \delta^{s's'''} \delta^{s''s'} + \sum_{m=1}^3 \left(\frac{\sigma^m}{2} \right)^{s's'''} \left(\frac{\sigma^m}{2} \right)^{s''s'}, \quad (\text{A.4})$$

$$\frac{1}{2}\delta_{mk}\delta_{i\ell} = \frac{1}{2N}\delta_{m\ell}\delta_{ik} + \sum_{\alpha=1}^{N^2-1} \left(\frac{\lambda^\alpha}{2}\right)_{m\ell} \left(\frac{\lambda^\alpha}{2}\right)_{ik}, \quad (\text{A.5})$$

$$\text{tr} \frac{\lambda^\alpha}{2} \frac{\lambda^\beta}{2} = \frac{1}{2}\delta^{\alpha\beta} \text{ etc.}$$

Since we will only consider condensates of flavor/spin singlet excitons, we shall keep here only the first terms in the r.h.s. of eqs. (A.4) and (A.5) and discard the other ones.

Expression (A.3) then simplifies to the form

$$[\bar{\psi}M\psi][\bar{\psi}N\psi] = -\frac{1}{16N_f} (\text{Tr}M\Gamma^A N\Gamma^B) [\bar{\psi}\Gamma^B\psi][\bar{\psi}\Gamma^A\psi], \quad (\text{A.6})$$

with $N_f = 2N$, $[\bar{\psi}M\psi] = \bar{\psi}^{as}M\psi^{as}$ etc., and a summation over repeated spin/flavor indices (s, a) is understood. Obviously, in our case we have $M = N$, and we have to apply eq.(A.3) for $M \otimes M = \{\gamma^0 \otimes \gamma^0, t^0 \otimes t^0\}$. In order to quote the required Fierz-transformed expressions, it is convenient to introduce the following notations:

$$\begin{aligned} \vec{V} &= \{\bar{\psi}\Gamma_i\psi\}, \quad \Gamma_i = \{\mathbb{I}_4, \gamma^3, i\gamma^5\}, \quad S = \bar{\psi}\gamma^{35}\psi, \\ \vec{V}^\mu &= \{\bar{\psi}\gamma^\mu\Gamma_i^*\psi\}, \quad \Gamma_i^* = \{\mathbb{I}_4, i\gamma^3, \gamma^5\}, \quad S^\mu = \bar{\psi}\gamma^\mu\gamma^{35}\psi, \end{aligned} \quad (\text{A.7})$$

(Note that Γ_i^* is not the conjugate of Γ_i .) For comparison, let us start with the Lorentz- and chiral invariant Thirring-like four-fermion term

$$(\bar{\psi}\gamma_\mu\psi)(\bar{\psi}\gamma^\mu\psi) = -\frac{1}{4N_f} \left\{ 3(\vec{V}^2 + S^2) - (\vec{V}_\mu \cdot \vec{V}^\mu + S_\mu S^\mu) \right\}. \quad (\text{A.8})$$

The Lorentz non-invariant, but chiral invariant Coulomb-type interaction and the chiral symmetry breaking Lorentz-invariant terms, considered in the text, transform as follows

$$[\bar{\psi}\gamma^0\psi][\bar{\psi}\gamma^0\psi] = -\frac{1}{4N_f} \left\{ (\vec{V}^2 + S^2) + \vec{V}^\mu \cdot \vec{V}^\mu + S^\mu S^\mu \right\}. \quad (\text{A.9})$$

$$[\bar{\psi}\psi][\bar{\psi}\psi] = -\frac{1}{4N_f} \left\{ (\vec{V}^{*2} + S^2) + \vec{V}^*_{\mu} \cdot \vec{V}^{*\mu} + S_\mu S^\mu \right\}. \quad (\text{A.10})$$

Here we used the notations

$$\begin{aligned} \vec{V}_\mu \cdot \vec{V}^\mu &= g_{\mu\nu} \vec{V}^\mu \cdot \vec{V}^\nu = \vec{V}^0 \cdot \vec{V}^0 - \vec{V}^i \cdot \vec{V}^i, \\ \vec{V}^\mu \cdot \vec{V}^\mu &= \vec{V}^0 \cdot \vec{V}^0 + \vec{V}^i \cdot \vec{V}^i, \text{ etc.}, \\ \vec{V}^* &= \{\bar{\psi}\Gamma_i^*\psi\}, \quad \vec{V}^{*\mu} = \{\bar{\psi}\gamma^\mu\Gamma_i\psi\}. \end{aligned} \quad (\text{A.11})$$

In the text we have only considered the NJL-type scalar/pseudoscalar interactions of flavor/spin-singlet type and discarded, for simplicity, non-singlet axial/vector type interactions.

Appendix B. Phase structure of the generalized Gross–Neveu model (37)

The phase structure of the schematic model (37) is described by the effective potential (56), where, for brevity of notations, we put here $\nu_F = 1$, and, for convenience, shift also the absolute value sign in the original definition of M_k to the term $|M_k|^3$

$$V(\sigma_i, \varphi_i) = \sum_{k=1}^2 \left[\frac{g_k}{4} \sigma_k^2 + \frac{h_k}{4} \varphi_k^2 + \frac{|M_k|^3}{6\pi} \right]. \quad (\text{B.1})$$

Thus we now have $M_1 = \sigma_2 + \sqrt{\sigma_1^2 + \varphi_1^2 + \varphi_2^2}$, $M_2 = \sigma_2 - \sqrt{\sigma_1^2 + \varphi_1^2 + \varphi_2^2}$. Since the function (B.1) is even with respect to each variable $\sigma_{1,2}$ and $\varphi_{1,2}$, i.e. it is invariant under each of the transformations $\sigma_1 \rightarrow -\sigma_1$, $\sigma_2 \rightarrow -\sigma_2$, $\varphi_1 \rightarrow -\varphi_1$, and $\varphi_2 \rightarrow -\varphi_2$, we can suppose that in eq. (B.1) $\varphi_{1,2} \geq 0$ and $\sigma_{1,2} \geq 0$. Our goal is to find the global minimum point (GMP) of the effective potential (B.1) vs $\varphi_{1,2} \geq 0$ and $\sigma_{1,2} \geq 0$. However, the structure of the function (B.1) tells us to use at the beginning another set of independent variables. Namely, it is convenient first to study its extremal properties in terms of M_1 , M_2 , x and y , where $x = \varphi_1^2$, $y = \varphi_2^2$, and then return to the original variables $\varphi_{1,2} \geq 0$ and $\sigma_{1,2} \geq 0$. Since $\sigma_1^2 = -x - y + (M_1 - M_2)^2/4$ and $\sigma_2^2 = (M_1 + M_2)^2/4$, we have instead of eq. (B.1) the following function

$$V(M_1, M_2, x, y) = \frac{g_1}{16}(M_1 - M_2)^2 + \frac{g_2}{16}(M_1 + M_2)^2 + \frac{h_1 - g_1}{4}x + \frac{h_2 - g_1}{4}y + \frac{|M_1|^3}{6\pi} + \frac{|M_2|^3}{6\pi}. \quad (\text{B.2})$$

Note, there are natural restrictions on the new variables, $M_1 \geq 0$, $-\infty < M_2 < \infty$, $x, y \geq 0$ and $x + y \leq (M_1 - M_2)^2/4$. In order to find the GMP of the function (B.2), we use the following strategy. First, we will minimize it (at fixed $M_{1,2}$) with respect to x and y by varying in the compact and closed domain $\omega = \{(x, y) : x, y \geq 0, x + y \leq (M_1 - M_2)^2/4\}$. Second, the obtained minimal expression of the effective potential will then be minimized over $M_{1,2}$. Since $V(M_1, M_2, x, y)$ is a linear function in both x and y , it is obvious that its least value on the triangle region ω is reached in one of the vertices of this triangle, i.e. in one of the points $(x_1 = 0, y_1 = 0)$, $(x_2 = (M_1 - M_2)^2/4, y_2 = 0)$ and $(x_3 = 0, y_3 = (M_1 - M_2)^2/4)$. There, the effective potential (B.2) takes the following values

$$V_I(M_1, M_2) \equiv V(M_1, M_2, x = 0, y = 0) = \frac{g_1}{16}(M_1 - M_2)^2 + \frac{g_2}{16}(M_1 + M_2)^2 + \frac{M_1^3}{6\pi} + \frac{|M_2|^3}{6\pi}, \quad (\text{B.3})$$

$$V_{II}(M_1, M_2) \equiv V\left(M_1, M_2, x = \frac{(M_1 - M_2)^2}{4}, y = 0\right) = \frac{h_1}{16}(M_1 - M_2)^2 + \frac{g_2}{16}(M_1 + M_2)^2 + \frac{M_1^3}{6\pi} + \frac{|M_2|^3}{6\pi}, \quad (\text{B.4})$$

$$V_{III}(M_1, M_2) \equiv V\left(M_1, M_2, x = 0, y = \frac{(M_1 - M_2)^2}{4}\right) = \frac{h_2}{16}(M_1 - M_2)^2 + \frac{g_2}{16}(M_1 + M_2)^2 + \frac{M_1^3}{6\pi} + \frac{|M_2|^3}{6\pi}. \quad (\text{B.5})$$

To compare the quantities (B.3)-(B.5), let us fix the value of the coupling constant g_1 and divide the plane of the couplings h_1 and h_2 into three regions *I*, *II* and *III* (see Fig. 5 for the case $g_1 > 0$), where $I = \{(h_1, h_2) : h_1 > g_1, h_2 > g_1\}$, $II = \{(h_1, h_2) : h_1 < g_1, h_2 > h_1\}$ and $III = \{(h_1, h_2) : h_2 < g_1, h_2 < h_1\}$. Then a direct comparison of the functions (B.3)-(B.5) shows that (i) in the region *I* the GMP of the effective potential (B.2) with respect to x and y is the point $(x_1 = 0, y_1 = 0)$, where the least value of $V(M_1, M_2, x, y)$ is equal to the function $V_I(M_1, M_2)$. (ii) If the

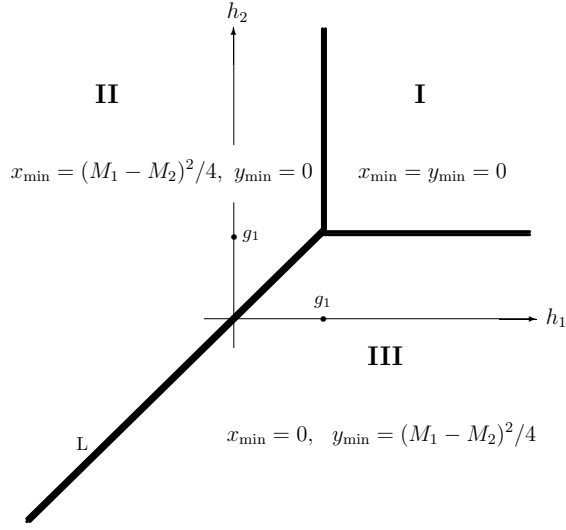


Figure B.5: The plane of coupling constants h_1 and h_2 is divided into three regions I, II and III. In each region the coordinates x_{\min} and y_{\min} of the least value point of the function (B.2) vs $(x, y) \in \omega = \{(x, y) : x, y \geq 0, x + y \leq (M_1 - M_2)^2/4\}$ are presented. The line L is defined by the relation $L \equiv \{(h_1, h_2) : h_1 = h_2\}$. For simplicity, the coupling constant g_1 is selected to be positive and determines here the origin (g_1, g_1) of the thick axis system.

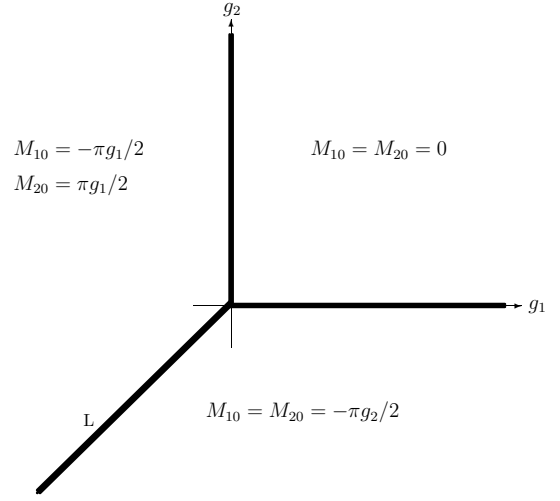


Figure B.6: The coordinates M_{10} and M_{20} of the global minimum point of the function $V_I(M_1, M_2)$ (B.3) in dependence on the coupling constants g_1, g_2 . The line L is defined by the relation $L \equiv \{(g_1, g_2) : g_1 = g_2\}$.

couplings h_1 and h_2 are in the region II, then the least value of the effective potential (B.2) vs x and y is reached at the point $(x_2 = (M_1 - M_2)^2/4, y_2 = 0)$, where it is the quantity $V_{II}(M_1, M_2)$. (iii) Finally, if $(h_1, h_2) \in III$, then the GMP of the function (B.2) over the variables x and y is realized at the point $(x_3 = 0, y_3 = (M_1 - M_2)^2/4)$ and the least value of (B.2) is the quantity $V_{III}(M_1, M_2)$. Now, we will find the GMPs of the functions $V_I(M_1, M_2)$, $V_{II}(M_1, M_2)$ and $V_{III}(M_1, M_2)$ vs M_1 and M_2 from the region $M_1 \geq 0, -\infty < M_2 < \infty$.

We start from the case, when $(h_1, h_2) \in I$, i.e. from finding of a GMP of the function $V_I(M_1, M_2)$. There is a system of two stationarity equations,

$$\begin{aligned} \frac{\partial V_I(M_1, M_2)}{\partial M_1} &\equiv \frac{g_1}{8}(M_1 - M_2) + \frac{g_2}{8}(M_1 + M_2) + \frac{M_1^2}{2\pi} = 0, \\ \frac{\partial V_I(M_1, M_2)}{\partial M_2} &\equiv \frac{g_1}{8}(M_2 - M_1) + \frac{g_2}{8}(M_1 + M_2) + \text{sign}(M_2) \frac{M_2^2}{2\pi} = 0, \end{aligned} \quad (\text{B.6})$$

where $\text{sign}(x)$ is the sign function. The GMP (M_{10}, M_{20}) of the function $V_I(M_1, M_2)$ is a solution of the system of stationarity equations (B.6). Moreover, it depends on the values of the coupling constants g_1 and g_2 . Solving the system (B.6), one can find the behavior of the coordinates M_{10} and M_{20} vs g_1 and g_2 (see Fig. 6, where the plane (g_1, g_2) is divided into three regions corresponding to different expressions for M_{10} and M_{20}). Namely, if $g_{1,2} > 0$, then $M_{10} = M_{20} = 0$. If $g_2 < 0$ and $g_2 < g_1$, then $M_{10} = M_{20} = -\pi g_2/2$. If $g_1 < 0$ and $g_2 > g_1$, then $M_{10} = -M_{20} = -\pi g_1/2$. Hence, returning to the original variables $\varphi_{1,2} \geq 0$ and $\sigma_{1,2} \geq 0$, one can establish the GMP of the effective potential

(B.1) and, as a result, the form of the ground state expectation values $\langle\sigma_{1,2}\rangle, \langle\varphi_{1,2}\rangle$ when $(h_1, h_2) \in I$. So we find that if

$$(g_1, g_2, h_1, h_2) \in \Omega_{I0} \equiv \{(g_1, g_2, h_1, h_2) : h_1 > g_1, h_2 > g_1; g_1 > 0, g_2 > 0\}, \quad (\text{B.7})$$

then all ground state expectation values are zero, $\langle\sigma_{1,2}\rangle = 0$ and $\langle\varphi_{1,2}\rangle = 0$. If

$$(g_1, g_2, h_1, h_2) \in \Omega_{I\sigma_1} \equiv \{(g_1, g_2, h_1, h_2) : h_1 > g_1, h_2 > g_1; g_1 < 0, g_2 > g_1\}, \quad (\text{B.8})$$

then $\langle\sigma_1\rangle = -\pi g_1/2, \langle\sigma_2\rangle = 0, \langle\varphi_{1,2}\rangle = 0$. Finally, if

$$(g_1, g_2, h_1, h_2) \in \Omega_{I\sigma_2} \equiv \{(g_1, g_2, h_1, h_2) : h_1 > g_1, h_2 > g_1; g_2 < 0, g_2 < g_1\}, \quad (\text{B.9})$$

then $\langle\sigma_2\rangle = -\pi g_2/2, \langle\sigma_1\rangle = 0, \langle\varphi_{1,2}\rangle = 0$.

If the point (h_1, h_2) belongs to the region *II*, then we need to study the extrema properties of the function $V_{II}(M_1, M_2)$. Since this function is obtained from (B.3) by the replacement $g_1 \rightarrow h_1$, the behavior of its GMP vs h_1 and g_2 can be easily found from Fig. 6 also by an evident replacement $g_1 \rightarrow h_1$. After that it is possible to get the form of ground state expectation values of the fields $\varphi_{1,2}$ and $\sigma_{1,2}$. Namely, if

$$(g_1, g_2, h_1, h_2) \in \Omega_{II0} \equiv \{(g_1, g_2, h_1, h_2) : h_1 < g_1, h_2 > h_1; h_1 > 0, g_2 > 0\}, \quad (\text{B.10})$$

then $\langle\sigma_{1,2}\rangle = 0$ and $\langle\varphi_{1,2}\rangle = 0$. If

$$(g_1, g_2, h_1, h_2) \in \Omega_{II\varphi_1} \equiv \{(g_1, g_2, h_1, h_2) : h_1 < g_1, h_2 > h_1; h_1 < 0, g_2 > h_1\}, \quad (\text{B.11})$$

we have $\langle\sigma_1\rangle = \langle\sigma_2\rangle = 0, \langle\varphi_1\rangle = -\pi h_1/2, \langle\varphi_2\rangle = 0$. If

$$(g_1, g_2, h_1, h_2) \in \Omega_{II\sigma_2} \equiv \{(g_1, g_2, h_1, h_2) : h_1 < g_1, h_2 > h_1; g_2 < 0, g_2 < h_1\}, \quad (\text{B.12})$$

then $\langle\sigma_2\rangle = -\pi g_2/2, \langle\sigma_1\rangle = 0, \langle\varphi_{1,2}\rangle = 0$. In a similar way it is easy to establish the structure of the condensates $\langle\sigma_{1,2}\rangle$ and $\langle\varphi_{1,2}\rangle$ in the case when the point (h_1, h_2) belongs to the region *III*. So, we see that if

$$(g_1, g_2, h_1, h_2) \in \Omega_{III0} \equiv \{(g_1, g_2, h_1, h_2) : h_2 < g_1, h_2 < h_1; h_2 > 0, g_2 > 0\}, \quad (\text{B.13})$$

then $\langle\sigma_{1,2}\rangle = 0$ and $\langle\varphi_{1,2}\rangle = 0$. If

$$(g_1, g_2, h_1, h_2) \in \Omega_{III\varphi_2} \equiv \{(g_1, g_2, h_1, h_2) : h_2 < g_1, h_2 < h_1; h_2 < 0, g_2 > h_2\}, \quad (\text{B.14})$$

we have $\langle\sigma_1\rangle = \langle\sigma_2\rangle = 0, \langle\varphi_2\rangle = -\pi h_2/2, \langle\varphi_1\rangle = 0$. Finally, if

$$(g_1, g_2, h_1, h_2) \in \Omega_{III\sigma_2} \equiv \{(g_1, g_2, h_1, h_2) : h_2 < g_1, h_2 < h_1; g_2 < 0, g_2 < h_2\}, \quad (\text{B.15})$$

then $\langle\sigma_2\rangle = -\pi g_2/2, \langle\sigma_1\rangle = 0, \langle\varphi_{1,2}\rangle = 0$.

(g_1, g_2, h_1, h_2)	$\langle\sigma_1\rangle$	$\langle\sigma_2\rangle$	$\langle\varphi_1\rangle$	$\langle\varphi_2\rangle$
$(g_1, g_2, h_1, h_2) \in \Omega_{I0} \cup \Omega_{II0} \cup \Omega_{III0}$	0	0	0	0
$(g_1, g_2, h_1, h_2) \in \Omega_{I\sigma_1}$	$-\pi g_1/2$	0	0	0
$(g_1, g_2, h_1, h_2) \in \Omega_{I\sigma_2} \cup \Omega_{II\sigma_2} \cup \Omega_{III\sigma_2}$	0	$-\pi g_2/2$	0	0
$(g_1, g_2, h_1, h_2) \in \Omega_{II\varphi_1}$	0	0	$-\pi h_1/2$	0
$(g_1, g_2, h_1, h_2) \in \Omega_{III\varphi_2}$	0	0	0	$-\pi h_2/2$

Table B.2: The values of the condensates $\langle\sigma_1\rangle$, $\langle\sigma_2\rangle$, $\langle\varphi_1\rangle$ and $\langle\varphi_2\rangle$ in dependence on the coupling constants g_1 , g_2 , h_1 and h_2 . The regions $\Omega_{I0}, \dots, \Omega_{III\varphi_2}$ are defined in (B.7), ..., (B.15), correspondingly.

We summarize the results of our investigation of the effective potential (B.1) in the Table B.2. (Note that in order to apply the data of this table to the model (37) and/or to the effective potential (56), one should perform the replacements $g_i \rightarrow g_i v_F$ and $h_i \rightarrow h_i v_F$ there.) Each nontrivial combination of condensates $\langle\sigma_{1,2}\rangle$ and $\langle\varphi_{1,2}\rangle$, listed in Table B.2, corresponds to some broken discrete symmetries from the set $\{\mathcal{P}, \mathcal{C}, \mathcal{T}, \gamma^5, \gamma^3\}$, i.e. to some nontrivial phase of the model. The list of all possible phases of the model (37), including the trivial phase with $\langle\sigma_{1,2}\rangle = 0$ and $\langle\varphi_{1,2}\rangle = 0$, can be easily established with the help of Tables 1 and B.2 (see also the symmetry properties of the condensates in Sect. 2.4).

Appendix C. Calculations of the 1PI Green functions (65)

Choosing e.g. $\hat{t}_k = I_4$ in eq. (63), we have for the 1PI 2-point Green function $\Gamma_{\sigma_1\sigma_1}(x-y)$ of $\sigma_1(x)$ and $\sigma_1(y)$ fields the following expression

$$\Gamma_{\sigma_1\sigma_1}(z) \equiv \frac{\delta^2 S_{\text{eff}}^{(2)}}{\delta\sigma_1(x)\delta\sigma_1(y)} = -\frac{1}{2v_F G_1} \delta^{(3)}(z) + i \text{Tr}_s [G_0(z)G_0(-z)], \quad (\text{C.1})$$

where $z = x - y$ and the matrix elements of the propagator $G_0(z)$ are presented in eq. (64). Introducing the momentum-space representation $\Gamma_{\sigma_1\sigma_1}(p)$ for the Green function (C.1)

$$\Gamma_{\sigma_1\sigma_1}(p) = \int d^3z \Gamma_{\sigma_1\sigma_1}(z) e^{ipz}, \quad (\text{C.2})$$

and applying the corresponding Fourier transformation to both sides of eq. (C.1), using there the expression (64), one can find

$$\Gamma_{\sigma_1\sigma_1}(p) = -\frac{1}{2v_F G_1} + i \int \frac{d^3k}{(2\pi)^3} \text{Tr}_s \left[\left(\frac{1}{\vec{k} + \vec{p} - \langle\sigma_1\rangle} \right) \left(\frac{1}{\vec{k} - \langle\sigma_1\rangle} \right) \right]. \quad (\text{C.3})$$

It is clear from the stationarity equations for the effective potential (53) that

$$\frac{1}{2v_F G_1} = i \int \frac{d^3k}{(2\pi)^3} \frac{4}{\vec{k}^2 - \langle\sigma_1\rangle^2} \quad (\text{C.4})$$

in the case $\langle\sigma_1\rangle \neq 0$, $\langle\sigma_2\rangle = 0$, $\langle\varphi_1\rangle = 0$ and $\langle\varphi_2\rangle = 0$. Using eq. (C.4) in the expression (C.3), we have after trace calculation:

$$\Gamma_{\sigma_1\sigma_1}(p) = i \int \frac{d^3k}{(2\pi)^3} \left[\frac{-4\vec{p}^2 - 4\vec{k}\vec{p} + 8\langle\sigma_1\rangle^2}{(\vec{k}^2 - \langle\sigma_1\rangle^2)((\vec{k} + \vec{p})^2 - \langle\sigma_1\rangle^2)} \right]. \quad (\text{C.5})$$

Let us apply in eq. (C.5) the general relation

$$\frac{1}{AB} = \int_0^1 d\alpha \frac{1}{[A\alpha + B(1-\alpha)]^2}. \quad (\text{C.6})$$

Then we have:

$$\begin{aligned} \Gamma_{\sigma_1\sigma_1}(p) &= i \int_0^1 d\alpha \int \frac{d^3k}{(2\pi)^3} \frac{-4\tilde{p}^2 - 4\tilde{k}\tilde{p} + 8\langle\sigma_1\rangle^2}{[(\tilde{k}^2 - \langle\sigma_1\rangle^2)\alpha + ((\tilde{k} + \tilde{p})^2 - \langle\sigma_1\rangle^2)(1-\alpha)]^2} \\ &= i \int_0^1 d\alpha \int \frac{d^3k}{(2\pi)^3} \frac{-4\tilde{p}^2 - 4\tilde{k}\tilde{p} + 8\langle\sigma_1\rangle^2}{[\tilde{p}^2\alpha(1-\alpha) + (\tilde{k} + \alpha\tilde{p})^2 - \langle\sigma_1\rangle^2]^2}. \end{aligned} \quad (\text{C.7})$$

Now let us change variables in the k -integration in eq. (C.7), $q = k + \alpha p$. Then

$$\begin{aligned} \Gamma_{\sigma_1\sigma_1}(p) &= i \int_0^1 d\alpha \int \frac{d^3q}{(2\pi)^3} \frac{-4\tilde{p}^2(1-\alpha) - 4\tilde{q}\tilde{p} + 8\langle\sigma_1\rangle^2}{[\tilde{q}^2 + \tilde{p}^2\alpha(1-\alpha) - \langle\sigma_1\rangle^2]^2} \\ &= i \int_0^1 d\alpha \int \frac{d^3q}{(2\pi)^3} \frac{-4\tilde{p}^2(1-\alpha) + 8\langle\sigma_1\rangle^2}{[\tilde{q}^2 + \tilde{p}^2\alpha(1-\alpha) - \langle\sigma_1\rangle^2]^2}. \end{aligned} \quad (\text{C.8})$$

Note that in the second line of this equation we have ignored in the numerator of the fraction the linear term in \tilde{q} , which evidently does not contribute to the q integration in eq. (C.8).

Suppose now that $\tilde{p}^2 < 0$ in eq. (C.8). In this case one can perform in eq. (C.8) a Wick rotation of the q_0 -integration contour and change variables there, $q_0 \rightarrow iq_0$, $q_1 \rightarrow q_1/v_F$ and $q_2 \rightarrow q_2/v_F$. As a result, we obtain the integration over 3-dim Euclidean q -momentum space. Using in the q -integral the polar coordinate system, where $\int d^3q = 4\pi \int x^2 dx$ and $x = \sqrt{q_0^2 + q_1^2 + q_2^2}$, we have

$$\Gamma_{\sigma_1\sigma_1}(p) = -\frac{1}{v_F^2} \int_0^1 d\alpha [-4\tilde{p}^2(1-\alpha) + 8\langle\sigma_1\rangle^2] \int_0^\infty \frac{dx}{2\pi^2} \frac{x^2}{[x^2 + \mu^2]^2}, \quad (\text{C.9})$$

where $\mu^2 = -\tilde{p}^2\alpha(1-\alpha) + \langle\sigma_1\rangle^2$. The integration over x in eq. (C.9) is trivial, so

$$\Gamma_{\sigma_1\sigma_1}(p) = -\frac{1}{8\pi v_F^2} \int_0^1 d\alpha \frac{-4\tilde{p}^2(1-\alpha) + 8\langle\sigma_1\rangle^2}{\sqrt{-\tilde{p}^2\alpha(1-\alpha) + \langle\sigma_1\rangle^2}}. \quad (\text{C.10})$$

To integrate in eq. (C.10) one can use the substitution $\alpha = \beta + 1/2$. Note that in the obtained integral we can ignore again in the numerator of the fraction the linear over β term, so

$$\Gamma_{\sigma_1\sigma_1}(p) = -\frac{1}{8\pi v_F^2} \int_{-1/2}^{1/2} d\beta \frac{-2\tilde{p}^2 + 8\langle\sigma_1\rangle^2}{\sqrt{-\tilde{p}^2} \sqrt{a^2 - \beta^2}}, \quad (\text{C.11})$$

where $a^2 = [\langle\sigma_1\rangle^2 - \tilde{p}^2/4] / (-\tilde{p}^2) = 1/4 - \langle\sigma_1\rangle^2/\tilde{p}^2$ (Note, $a^2 > 1/4$). Hence,

$$\Gamma_{\sigma_1\sigma_1}(p) = \frac{\tilde{p}^2 - 4\langle\sigma_1\rangle^2}{4\pi v_F^2 \sqrt{-\tilde{p}^2}} \arcsin\left(\frac{\beta}{a}\right) \Big|_{\beta=-1/2}^{\beta=1/2} = \frac{\tilde{p}^2 - 4\langle\sigma_1\rangle^2}{2\pi v_F^2 \sqrt{-\tilde{p}^2}} \arcsin\left(\frac{1}{2a}\right). \quad (\text{C.12})$$

Finally, in order to obtain the expression (65) for $\Gamma_{\sigma_1\sigma_1}(p)$, it is necessary to use in eq. (C.12) the identity

$$\arcsin x = \arctan\left(\frac{x}{\sqrt{1-x^2}}\right). \quad (\text{C.13})$$

In a similar way one can obtain the expressions for the other 1PI Green functions of eq. (65). For example, to find $\Gamma_{\varphi_1\varphi_1}(p)$, we should use in eq. (63) the substitution $\hat{t}_k = i\gamma^5$. Then, by analogy with eq. (C.3), we have

$$\Gamma_{\varphi_1\varphi_1}(p) = -\left(\frac{1}{2v_F H_1} - \frac{1}{2v_F G_1}\right) - \frac{1}{2v_F G_1} - i \int \frac{d^3k}{(2\pi)^3} \text{Tr}_s \left[\left(\frac{1}{\bar{k} + \bar{p} - \langle\sigma_1\rangle} \right) \gamma^5 \left(\frac{1}{\bar{k} - \langle\sigma_1\rangle} \right) \gamma^5 \right]. \quad (\text{C.14})$$

Due to the relations (57) for bare coupling constants G_1 and H_1 , the expression in the first round brackets in eq. (C.14) is equal to $(h_1 - g_1)/2v_F$. Taking into account eq. (C.4), the sum of other terms in eq. (C.14) brings us to the following expression

$$\Gamma_{\varphi_1\varphi_1}(p) = -\frac{h_1 - g_1}{2v_F} + i \int \frac{d^3k}{(2\pi)^3} \left[\frac{-4\bar{p}^2 - 4\bar{k}\bar{p}}{(\bar{k}^2 - \langle\sigma_1\rangle^2)((\bar{k} + \bar{p})^2 - \langle\sigma_1\rangle^2)} \right]. \quad (\text{C.15})$$

Applying in eq. (C.15) the α -representation formula (C.6), we obtain after several variable changes both in the k -integration, $k = q - \alpha p$, and then in the α -integration, $\alpha = \beta + 1/2$, the following expression

$$\Gamma_{\varphi_1\varphi_1}(p) = -\frac{h_1 - g_1}{2v_F} - 2i\bar{p}^2 \int_{\beta=-1/2}^{\beta=1/2} d\beta \int \frac{d^3q}{(2\pi)^3} \frac{1}{[\bar{q}^2 + \bar{p}^2(1/4 - \beta^2) - \langle\sigma_1\rangle^2]^2}. \quad (\text{C.16})$$

It can be evaluated by using the Wick-rotation technique, which results in two table integrations both over q and β (similar calculations are presented after eq. (C.8)). As a result, we obtain the 2-point 1PI Green function of the φ_1 fields (65).

In a similar way it is possible to get the expressions (65) for $\Gamma_{\varphi_2\varphi_2}(p)$ and $\Gamma_{\sigma_2\sigma_2}(p)$.

References

References

- [1] see e.g.: E. Fradkin, "Field Theories of Condensed Matter Systems", Addison-Wesley Publishing Company, 1991; Naoto Nagaosa "Quantum Field Theory in Condensed Matter Physics", Springer, 1999.
- [2] A.J. Heeger, S. Kivelson, J.R. Schrieffer, and W.-P. Su, Rev. Mod. Phys. **60**, 781 (1988), DOI:10.1103/RevModPhys.60.781.
- [3] D.K. Campbell, Nucl. Phys. B **200**[FS4], 297 (1982), DOI:10.1016/0550-3213(82)90089-X.
- [4] V. Schön and M. Thies, At the Frontier of Particle Physics: Handbook of QCD: "Boris Ioffe Festschrift", Vol. **3**, 1945, World Scientific (2001), arXiv:hep-th/0008175;
- [5] A.H.C. Neto, F. Guinea, N.M.R. Peres, K.S. Novoselov, and A.K. Geim, Rev. Mod. Phys. **81**, 109 (2009), DOI:10.1103/RevModPhys.81.109, arXiv:0709.1163, and references therein; concerning the experimental realization see also: K.S. Novoselov, A.K. Geim, S.V. Morozov, D. Jiang, Y. Zhang, S.V. Dubonos, I.V. Grigorieva, and A.A. Firsov, Science **306**, 666 (2004), DOI:10.1126/science.1102896, arXiv:cond-mat/0410550; K.S. Novoselov, A.K. Geim, S.V. Morozov, D. Jiang, M.I. Katsnelson, I.V. Grigorieva, S.V. Dubonos, and A.A. Firsov, Nature (London) **438**, 197 (2005), DOI:10.1038/nature04233, arXiv:cond-mat/0509330.
- [6] P.R. Wallace, Phys. Rev. **71**, 622 (1947), DOI:10.1103/PhysRev.71.622.
- [7] V.P. Gusynin, S.G. Sharapov, and J.P. Carbotte, Int. J. Mod. Phys. B **21**, 4611 (2007), DOI:10.1142/S0217979207038022, arXiv:0706.3016.
- [8] Y. Nambu and G. Jona-Lasinio, Phys. Rev. **122**, 345 (1961), DOI:10.1103/PhysRev.122.345; Phys. Rev. **124**, 246 (1961), DOI:10.1103/PhysRev.124.246.
- [9] J. Bardeen, L.N. Cooper, and J.R. Schrieffer, Phys. Rev. **108**, 1175 (1957), DOI:10.1103/PhysRev.108.1175.

- [10] N.N. Bogoliubov, J. Exptl. Theoret. Physics (U.S.S.R.) **34**, 58, 73 (1958) [Soviet Phys.-JETP **34**, 41, 51 (1958)].
- [11] D. Ebert and H. Reinhardt, Nucl. Phys. B **271**, 188 (1986), DOI:10.1016/S0550-3213(86)80009-8;
D. Ebert, H. Reinhardt, and M.K. Volkov, Progr. Part. Nucl. Phys. **33**, 1 (1994), DOI:10.1016/0146-6410(94)90043-4.
- [12] D.J. Gross and A. Neveu, Phys. Rev. D **10**, 3235 (1974), DOI:10.1103/PhysRevD.10.3235.
- [13] K.G. Klimenko, Z. Phys. C **37**, 457 (1988), DOI:10.1007/BF01578141;
B. Rosenstein, B.J. Warr, and S.H. Park, Phys. Rev. D **39**, 3088(1989), DOI:10.1103/PhysRevD.39.3088; Phys. Rev. Lett. **62**, 1433 (1989), DOI:10.1103/PhysRevLett.62.1433.
- [14] G.W. Semenoff and L.C.R. Wijewardhana, Phys. Rev. Lett. **63**, 2633 (1989) DOI:10.1103/PhysRevLett.63.2633; Phys. Rev. D **45**, 1342 (1992), DOI:10.1103/PhysRevD.45.1342.
- [15] B. Rosenstein, B.J. Warr and S.H. Park, Phys. Rept. **205**, 59 (1991), DOI:10.1016/0370-1573(91)90129-A.
- [16] H. Caldas and R.O. Ramos, Phys. Rev. B **80**, 115428 (2009), DOI:10.1103/PhysRevB.80.115428, arXiv:0907.0723;
R.O. Ramos and P.H.A. Manso, Phys. Rev. D **87**, 125014 (2013), DOI:10.1103/PhysRevD.87.125014, arXiv:1303.5463;
K.G. Klimenko and R.N. Zhokhov, Phys. Rev. D **88**, 105015 (2013), DOI:10.1103/PhysRevD.88.105015, arXiv:1307.7265.
- [17] A.S. Vshivtsev, B.V. Magnitsky, V.Ch. Zhukovsky, and K.G. Klimenko, Phys. Part. Nucl. **29**, 523 (1998), DOI:10.1134/1.953089.
- [18] D. Ebert, K.G. Klimenko, A.V. Tyukov, and V.Ch. Zhukovsky, Phys. Rev. D **78**, 045008 (2008), DOI:10.1103/PhysRevD.78.045008, arXiv:0804.4826.
- [19] D. Ebert, T.K. Khunjua, K.G. Klimenko, and V.Ch. Zhukovsky, Int. J. Mod. Phys. A **27**, 1250162 (2012), DOI:10.1142/S0217751X1250162X, arXiv:1106.2928.
- [20] J.E. Drut and D.T. Son, Phys. Rev. B **77**, 075115 (2008), DOI:10.1103/PhysRevB.77.075115, arXiv:0710.1315.
- [21] V. Juricic, I.F. Herbut, and G.W. Semenoff, Phys. Rev. B **80**, 081405(R) (2009), DOI:10.1103/PhysRevB.80.081405, arXiv:0906.3513;
I.F. Herbut, V. Juricic, and O. Vafek, Phys. Rev. B **80**, 075432 (2009), DOI:10.1103/PhysRevB.80.075432, arXiv:0904.1019.
- [22] G.W. Semenoff, Phys. Scr. T **146**, 014016 (2012), DOI:10.1088/0031-8949/2012/T146/014016, arXiv:1108.2945.
- [23] O.V. Gamayun, E.V. Gorbar and V.P. Gusynin, Phys. Rev. B **81**, 075429 (2010), DOI:10.1103/PhysRevB.81.075429, arXiv:0911.4878.
- [24] C. Popovici, C.S. Fischer, and L. von Smekal, Phys. Rev. B **88**, 205429 (2013), DOI:10.1103/PhysRevB.88.205429, arXiv:1308.6199.
- [25] D. Mesterhazy, J. Berges, and L. von Smekal, Phys. Rev. B **86**, 245431 (2012), DOI:10.1103/PhysRevB.86.245431, arXiv:1207.4054.
- [26] L. Janssen and H. Gies, Phys. Rev. D **86**, 105007 (2012), DOI:10.1103/PhysRevD.86.105007, arXiv:1208.3327.
- [27] Y. Aharonov and D. Bohm, Phys. Rev. **115**, 485 (1959), DOI:10.1103/PhysRev.115.485.
- [28] E.V. Gorbar, V.P. Gusynin and V.A. Miransky, Phys. Rev. D **64**, 105028 (2001), DOI:10.1103/PhysRevD.64.105028, arXiv:hep-ph/0105059.
- [29] I.F. Herbut, V. Juricic, and B. Roy, Phys. Rev. B **79**, 085116 (2009), DOI:10.1103/PhysRevB.79.085116, arXiv:0811.0610.
- [30] J. Alicea and M.P.A. Fisher, Phys. Rev. B **74**, 075422 (2006), DOI:10.1103/PhysRevB.74.075422, arXiv:cond-mat/0604601.
- [31] T.O. Wehling et.al., Phys. Rev. Lett. **106**, 236805 (2011), DOI:10.1103/PhysRevLett.106.236805, arXiv:1101.4007.
- [32] K.G. Klimenko, Z. Phys. C **57**, 175 (1993), DOI:10.1007/BF01555750; Theor. Mat. Phys. **94**, 393 (1993) [Teor. Mat. Fiz. **95**, 42 (1993)], DOI:10.1007/BF01016999.
- [33] D.Y. Song, Phys. Rev. D **48**, 3925 (1993), DOI:10.1103/PhysRevD.48.3925.
- [34] O.V. Gamayun and E.V. Gorbar, Phys. Lett. B **610**, 74 (2005), DOI:10.1016/j.physletb.2005.01.079, arXiv:hep-ph/0411157.
- [35] V.Ch. Zhukovsky and E.A. Stepanov, Phys. Lett. B **718**, 597 (2012), DOI:10.1016/j.physletb.2012.10.039.
- [36] D. Ebert, T.G. Khunjua, K.G. Klimenko and V.Ch. Zhukovsky, Phys. Rev. D **91**, 105024 (2015), DOI:10.1103/PhysRevD.91.105024, arXiv:1504.02867.
- [37] D. Ebert, V.Ch. Zhukovsky, and A.V. Tyukov, Mod. Phys. Lett. A **25**, 2933 (2010), DOI:10.1142/S0217732310034249, arXiv:1007.0191.
- [38] I.V. Krive and S.A. Naftulin, Nucl. Phys. B **364**, 541 (1991), DOI:10.1016/0550-3213(91)90276-4.
- [39] N.A. Viet, H. Ajiki, and T. Ando, J. Phys. Soc. Jpn. **63**, 3036 (1994), DOI:10.1143/JPSJ.63.3036.

- [40] T. Ando, *J. Phys. Soc. Jpn.* **74**, 777 (2005), DOI:10.1143/JPSJ.74.777.
- [41] E. Elizalde, S.D. Odintsov, and A.A. Saharian, *Phys. Rev. D* **83**, 105023 (2011), DOI:10.1103/PhysRevD.83.105023, arXiv:1102.2202.
- [42] G.W. Semenoff, *Phys. Rev. Lett.* **53**, 2449 (1984), DOI:10.1103/PhysRevLett.53.2449.
- [43] D. Ebert, V.Ch. Zhukovsky and E.A. Stepanov, *J. Phys.: Condens. Matter* **26**, 125502 (2014), DOI:10.1088/0953-8984/26/12/125502, arXiv:1307.5422.
- [44] M.A.H. Vozmediano, M.I. Katsnelson, F. Guinea, *Phys. Rep.* **496**, 109 (2010), DOI:10.1016/j.physrep.2010.07.003, arXiv:1003.5179.
- [45] D.T. Son, *Phys. Rev. B* **75**, 235423 (2007), DOI:10.1103/PhysRevB.75.235423, arXiv:cond-mat/0701501.
- [46] E.V. Gorbar, V.P. Gusynin, V.A. Miransky, and I.A. Shovkovy, *Phys. Rev. B* **78**, 085437 (2008), DOI:10.1103/PhysRevB.78.085437, arXiv:0806.0846.
- [47] H. Gies and L. Janssen, *Phys. Rev. D* **82**, 085018 (2010), DOI:10.1103/PhysRevD.82.085018, arXiv:1006.3747.
- [48] V.A. Miransky, *Dynamical Symmetry Breaking in Quantum Field Theories* (World Scientific, Singapore, 1993).
- [49] G. Murthy and R. Shankar, *Rev. Mod. Phys.* **75**, 1101 (2003), DOI:10.1103/RevModPhys.75.1101; M.O. Goerbig, arXiv:0909.1998 (2009).
- [50] K.G. Klimenko, *Z. Phys. C* **54**, 323 (1992), DOI:10.1007/BF01566663; *Theor. Math. Phys.* **90**, 1 (1992), DOI:10.1007/BF01018812; V.Ch. Zhukovsky, K.G. Klimenko and V.V. Khudiyakov, *Theor. Math. Phys.* **124**, 1132 (2000) [*Teor. Mat. Fiz.* **124**, 323 (2000)], DOI:10.1007/BF02551083, arXiv:hep-ph/0010123; V.P. Gusynin, V.A. Miransky and I.A. Shovkovy, *Phys. Rev. Lett.* **73**, 3499 (1994), DOI:10.1103/PhysRevLett.73.3499, arXiv:hep-ph/9405262; I.A. Shovkovy, *Lect. Notes Phys.* **871**, 13 (2013), DOI:10.1007/978-3-642-37305-3_2, arXiv:1207.5081; V.A. Miransky and I.A. Shovkovy, *Phys. Rep.* **576**, 1 (2015), DOI:10.1016/j.physrep.2015.02.003, arXiv:1503.00732.
- [51] G.W. Semenoff, I.A. Shovkovy, and L.C.R. Wijewardhana, *Mod. Phys. Lett. A* **13**, 1143 (1998), DOI:10.1142/S0217732398001212, arXiv:hep-ph/9803371.
- [52] V.Ch. Zhukovsky, K.G. Klimenko, V.V. Khudiyakov and D. Ebert, *JETP Lett.* **73**, 121 (2001), DOI:10.1134/1.1364538, arXiv:hep-th/0012256; V.Ch. Zhukovsky and K.G. Klimenko, *Theor. Math. Phys.* **134**, 254 (2003), DOI:10.1023/A:1022284205855; E.J. Ferrer, V.P. Gusynin and V. de la Incera, *Mod. Phys. Lett. B* **16**, 107 (2002), DOI:10.1142/S0217984902003555, arXiv:hep-ph/0101308; *Eur. Phys. J. B* **33**, 397 (2003), DOI:10.1140/epjb/e2003-00181-8, arXiv:cond-mat/0203217.
- [53] F.D.M. Haldane, *Phys. Rev. Lett.* **61**, 2015 (1988), DOI:10.1103/PhysRevLett.61.2015.
- [54] J.-C. Charlier, X. Blase, S. Roche, *Rev. Mod. Phys.* **79**, 677 (2007), DOI:10.1103/RevModPhys.79.677.
- [55] D. Ebert and K.G. Klimenko, *Phys. Rev. D* **80**, 125013 (2009), DOI:10.1103/PhysRevD.80.125013, arXiv:0911.1944.
- [56] N.D. Mermin and H. Wagner, *Phys. Rev. Lett.* **17**, 1133 (1966), DOI:10.1103/PhysRevLett.17.1133; S. Coleman, *Commun. Math. Phys.* **31**, 259 (1973), DOI:10.1007/BF01646487.
- [57] E. Babaev, *Phys. Lett. B* **497**, 323 (2001), DOI:10.1016/S0370-2693(00)01335-6, arXiv:hep-th/9907089.
- [58] W. Bietenholz, A. Gfeller, and U.-J. Wiese, *JHEP* **0310**, 018 (2003), DOI:10.1088/1126-6708/2003/10/018, arXiv:hep-th/0309162.
- [59] V.Ch. Zhukovsky and P.B. Kolmakov, *Moscow Univ. Phys. Bull.* **68**, 272 (2013) [*Vestn. Mosk. Univ.* **2013**, no. **4**, 814 (2013)], DOI:10.3103/S0027134913040127.